Supporting Information

for

Hypoiodous Acid-Catalyzed Regioselective Geminal Addition of Methanol to Vinylarenes: Synthesis of anti-Markovnikov Methyl Acetals

Peraka Swamy,[a,b] Mameda Naresh,[a,b] Marri Mahender Reddy,[b] Kodumuri Srujana,[b] Chevella Durgaiah,[b] Sripadi Prabhakar[a,c] and Nama Narender*[a,b]

[a] Academy of Scientific and Innovative Research, CSIR-Indian Institute of Chemical Technology, Hyderabad 500 007, India
[b] I&PC Division, CSIR-Indian Institute of Chemical Technology, Hyderabad, Telangana, India-500 007
Tel.: +91–40-27191703; Fax: +91-40-27160387/27160757; E-mail: narendern33@yahoo.co.in; nama@iict.res.in
[c] NCMS, CSIR-Indian Institute of Chemical Technology, Hyderabad, Telangana, India-500 007

Table of contents

1. Experimental Section

1.1. General Information:

All chemicals (reagent grade) were purchased from Sigma-Aldrich and used as received without further purification. ^{1}H NMR spectra were recorded at 300 or 500 MHz and ^{13}C NMR spectra at 75 or 125 MHz in $CDCl_3$. The chemical shifts (δ) are reported in ppm units relative to TMS as an internal standard for ^{1}H NMR and $CDCl_3$ for ^{13}C NMR spectra. Coupling constants (*J*) are reported in hertz (Hz) and multiplicities are indicated as follows: s (singlet), br s (broad singlet), d (doublet), dd (doublet of doublet), m (multiplet). The UV-Vis absorption studies were carried out using Rayleigh (RAYLEIGH)UV-2100 spectrophotometer. The mass spectrometric analyses were carried out using High Resolution Q-TOF Mass Spectrometer. TLC inspections were performed on Silica gel 60 F_{254} plates. Column chromatography was performed on silica gel (100-200 mesh) using *n*-hexane-EtOAc as eluent.

1.2. General Procedure for the Metal-free Catalytic Addition of Methanol to Alkenes:

To a 25 mL of doubled necked round bottom flask charged with 5 mL of methanol was added NH_4I (20 mol%) and an alkene (1 mmol). The mixture was stirred for 1 min and the oxone® (1 mmol) was slowly added at 30 ^{o}C. The reaction mixture immediately acquires reddish brown colour (due to the formation of triiodide by the reaction of HOI with unreacted I^-) and was disappeared slowly upon stirring. The reaction was stopped after the completion of reaction (as indicated by TLC) or after further stirring for about 15 min from the regeneration of yellowish-orange colour (this colour is possibly due to the presence of HOI disproportionation products in the absence of oxidizable alkene moiety). The solvent was removed under reduced pressure and the product mixture was dissolved in ethyl acetate (25 mL). Then the organic product mixture was washed with distilled water (2x5 mL) and the organic layer was treated with 5% aqueous sodium thiosulfate solution (5 mL). Next, the organic layer was dried over anhydrous Na_2SO_4. The solvent was removed on vacuo and the residue was purified by column chromatography on silica gel using *n*-hexane-ethyl acetate as eluent.

2. Optimization study

Table S1. Optimization study for the iodide salt mediated metal-free catalytic addition of methanol to styrene (**1a**).[a],[b]

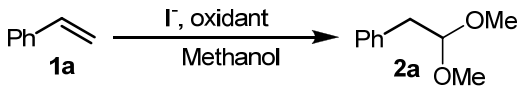

Entry	Iodide salt (mol %)	Oxone (equiv)	Temperature (^oC)	Time (h)	Yield (%)
1	NH_4I (20)	1	25 (RT)	12	71
2	NH_4I (20)	1	30	4.95	83
3	NH_4I (20)	1	50	2	56
4	NH_4I (30)	1	30	4.5	83
5	NH_4I (20)	1.5	30	3.5	54
6	NH_4I (20)	0.5	30	24	23
7	NH_4I (10)	1	30	12	63
8	TBAI (20)	1	30	5	79
9	KI (20)	1	30	5	79
10	CuI (20)	1	30	5	81
11	NH_4I (20)	1[c]	30	24	00
12	NH_4I (20)	1[d]	30	24	14
13	NH_4I (20)	1[e]	30	24	00
14	NH_4I (20)	1[f]	30	24	00
15	N/A[g]	1	30	24	00
16	20	N/A[g]	30	24	00

[a] Reaction conditions: styrene (1 mmol), iodide salt, oxone, methanol (5 mL). [b] Isolated yields. [c] $K_2S_2O_8$ was used as an oxidant instead of oxone. [d] *m*-CPBA was used as an oxidant instead of oxone. [e] aq.H_2O_2 was used as an oxidant instead of oxone. [f] aq.TBHP was used as an oxidant instead of oxone. [g] N/A refers to not applicable.

We initiated our investigation by choosing styrene as model substrate, NH_4I as pre-catalyst and a cheap, stable, non-toxic and non-nucleophilic oxone as terminal oxidant in methanol. Gratifyingly, the desired geminal dimethoxylation product, i.e., anti-Markovnikov methyl acetal (**2a**), was obtained in 71% yield at room temperature (Table S1, entry 1). When the reaction temperature was raised to 30 ^oC, the yield of the product was increased to 83% with decreased reaction time (Table S1, entry 2). But, the reaction at 50 ^oC diminishes the reaction time as well as yield of expected product (Table S1, entry 3). Either increasing or

decreasing of molar ratios of reagents could not improve the yield of **2a** (Table S1, entries 4-7). Next, we tested the various other iodide salts including TBAI, KI and CuI as pre-catalysts and we found that not one of the iodide salts was appropriate to increase the yield of desired product above that obtained for NH_4I (Table S1, entries 8-10). Further investigation showed that, the replacement of oxone with several oxidants such as $K_2S_2O_8$, *m*-CPBA, aq.H_2O_2 or aq. TBHP furnished the product **2a** albeit in low or zero yields (Table S1, entries 11-14). Finally, the role of the iodide salt and oxone in the reaction was established. When the reaction was performed in the absence of either iodine precursor or oxone, the reaction was unable to occur (Table S1, entries 15-16), which indicating that these reagents were essential for the reaction to proceed. After this extensive screening, we have observed that the 20 mol% of NH_4I and 1 equiv. of oxone with respect to **1a** at 30 ^oC were optimum to obtain the maximum yield of the desired product **2a** in methanol (Table S1, entry 2).

2. Mechanistic Investigations

To gain insight into the reaction pathway for the catalytic addition of methanol to vinylarenes, systematic investigations have been carried out and are described below.

2.1. Control Experiments

In order to establish the plausible reaction pathway, initially, we have performed several control experiments and are outlined in Scheme S1. The TLC inspections during the course of reaction of **1** under standard conditions indicated that the reaction proceeds through the formation of isolable intermediate, which is disappeared in TLC after completion of the reaction. In order to confirm the stable intermediate, the styrene acetalization reaction (model reaction of acetalization) was stopped at less than half of its original reaction time (Scheme S1, Eqn. 1) and column chromatographed to separate an intermediate and the product. These isolated compounds and above reaction mixture were analysed by GC-MS.

The GC chromatogram of the isolated intermediate contains an intense peak at t_R = 13.31 min and the product shows at t_R = 10.60 min (Figures S1-S2). The GC chromatogram of reaction mixture (Scheme S1, Eqn. 1) comprises two intense peaks at t_R = 10.55 min and t_R = 13.19 min (Figure S3). The EI mass spectrum of peak at t_R = 10.55 min exhibits the similar fragmentation pattern of (2,2-dimethoxyethyl)benzene (**2a**) (Figure S4) and the peak at t_R = 13.19 min shows analogous fragmentation behavior as 2-iodo-1-methoxy-1-phenylethane

(**3a**). Next, for further validation, the isolated intermediate (t_R = 10.60 min, Figure S1) and the product (t_R = 13.31 min, Figure S2) of styrene reaction were analyzed by NMR spectroscopy.

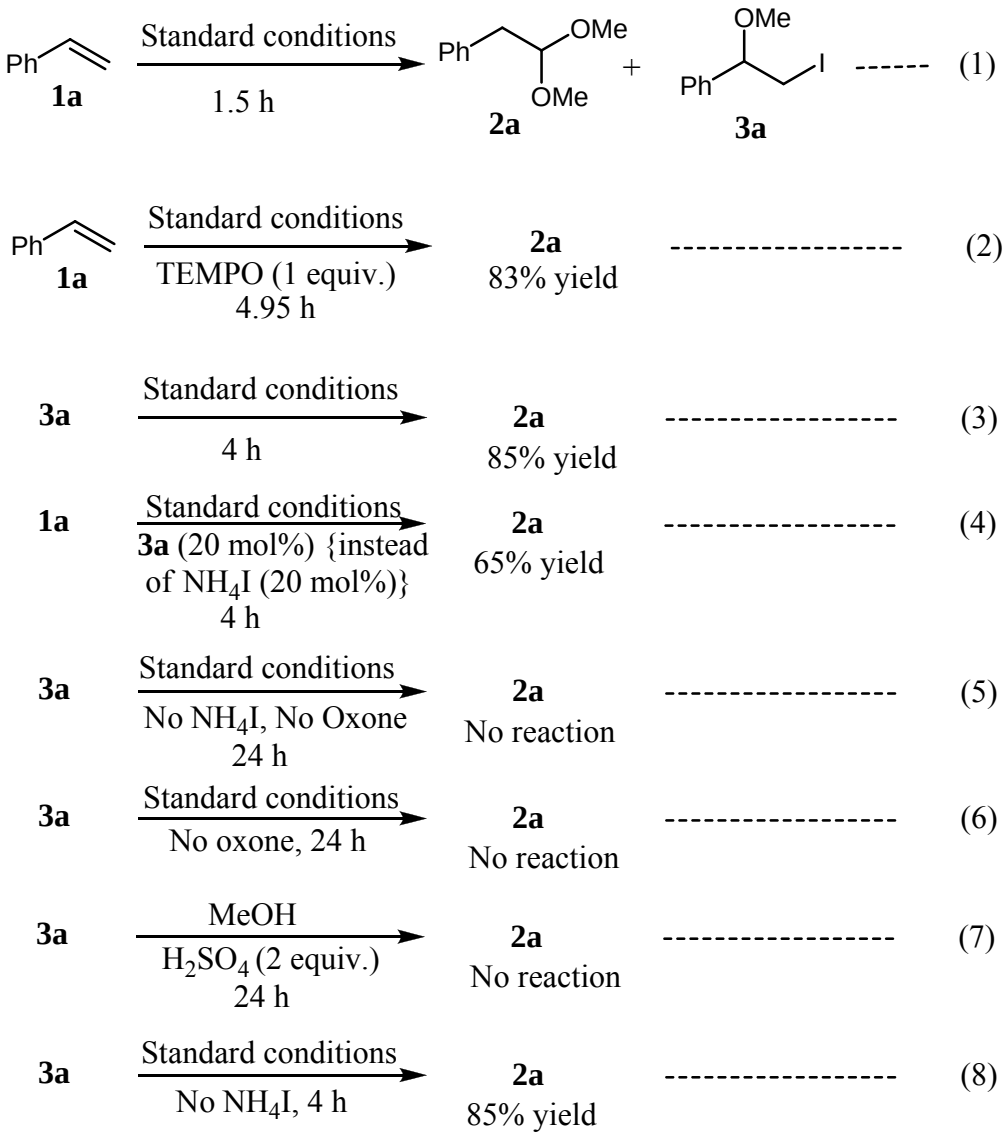

Scheme S1. Control experiments

The NMR (^{1}H and ^{13}C) spectrum of an intermediate contains signals (*see* Figure S6) as follows:

^{1}H NMR (500 MHz, $CDCl_3$): δ (ppm) = 7.43-7.28 (m, 5 H), 4.33-4.27 (m, 1 H), 3.39-3.31 (m, 2 H), 3.29 (s, 3 H). ^{13}C NMR (100 MHz, $CDCl_3$): δ (ppm) = 139.67, 128.60, 128.34, 126.45, 83.48, 57.22, 10.39. These values are very well in agreement with the reported values of 2-iodo-1-methoxy-1-phenylethane.[1]

The NMR (^{1}H and ^{13}C) spectrum of product contains signals (*see* Figure S7) as follows:

^{1}H NMR (500 MHz, $CDCl_3$): δ (ppm) = 7.33-7.26 (m, 2 H), 7.26-7.19 (m, 2 H), 4.54 (t, J = 5.64 Hz, 1 H), 3.33 (s, 6 H), 2.91 (d, J = 5.64 Hz, 2 H). ^{13}C NMR (125 MHz, $CDCl_3$): δ (ppm) = 136.95, 129.34, 128.25, 126.31, 105.23, 53.25, 39.58. These spectral data are in agreement with the reported values of (2,2-dimethoxyethyl)benzene.[2]

These GC-MS and NMR spectroscopy studies unambiguously confirming the isolated intermediate and product of styrene reaction (Scheme S1, Eqn.1) as **3a** and **2a**, respectively.

Figure S1. GC-EI total ion chromatogram of isolated intermediate of styrene reaction (Scheme S1, Eqn. 1)

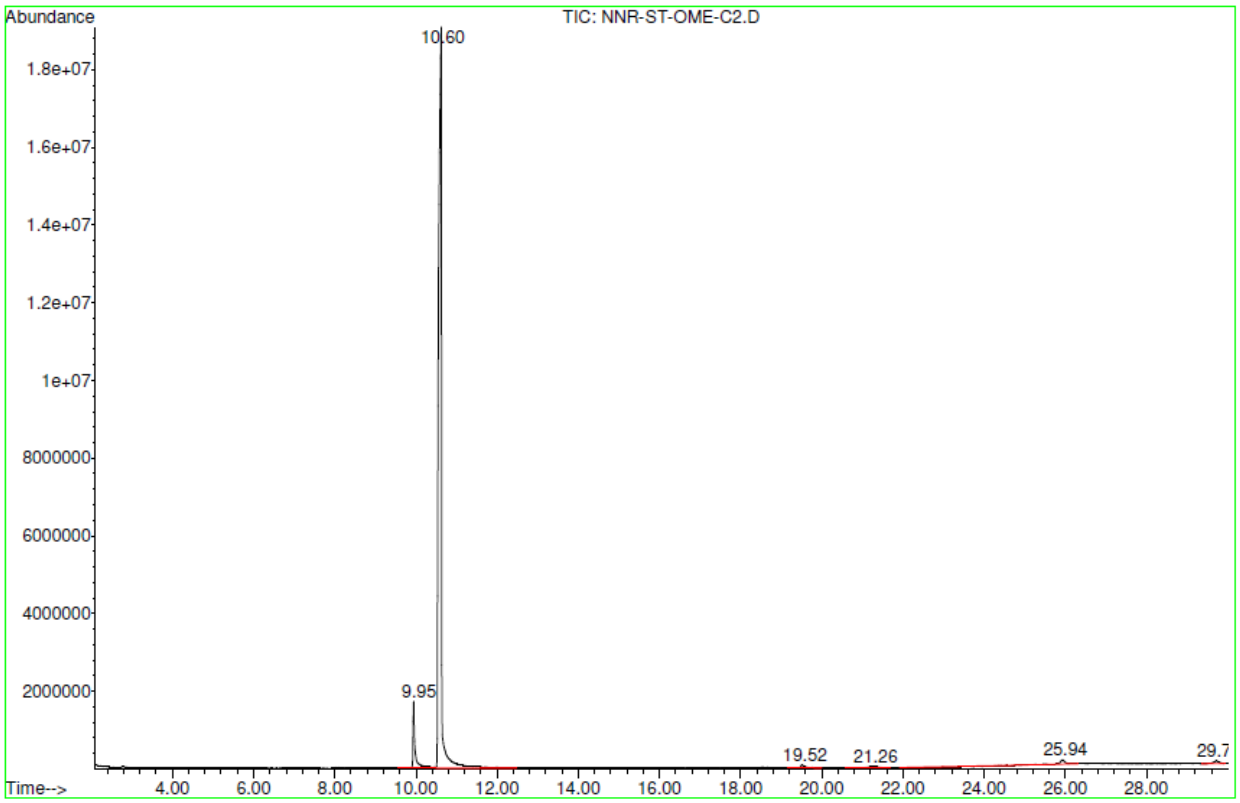

Figure S2. GC-MS total ion chromatogram of isolated product in styrene reaction (Scheme S1, Eqn. 1)

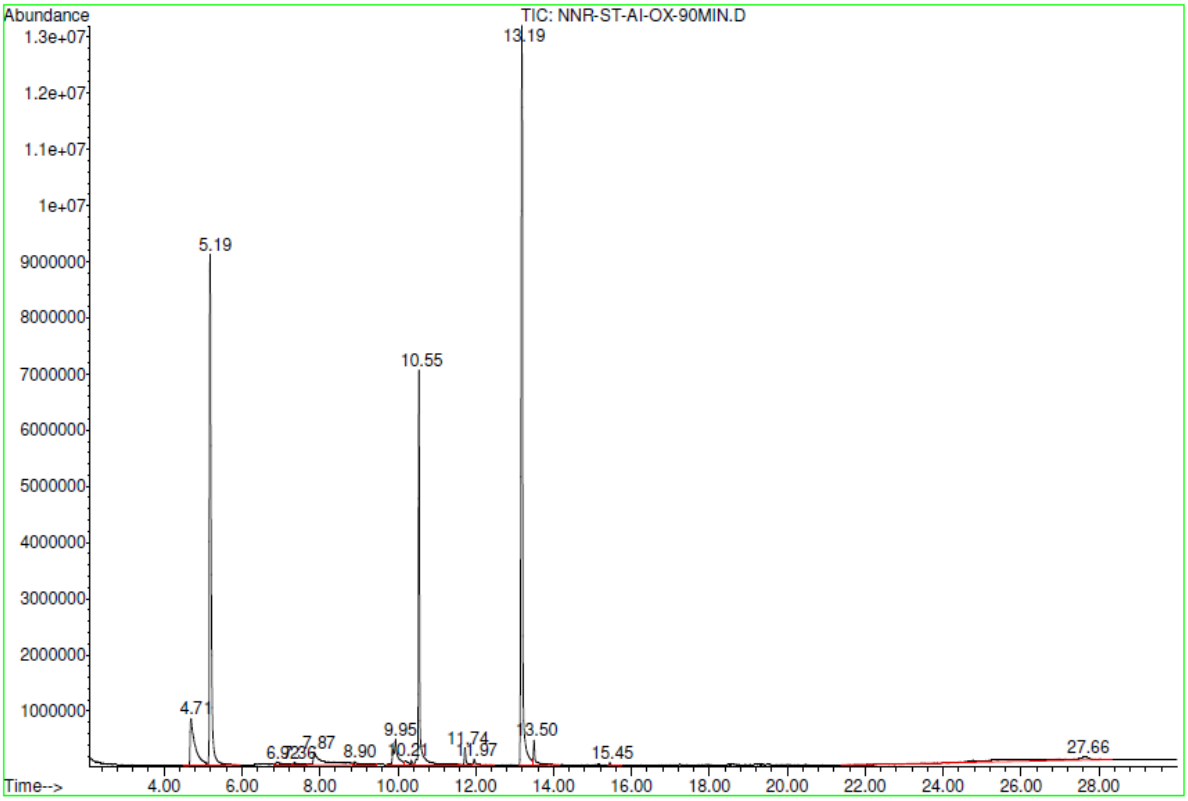

Figure S3. GC-EI total ion chromatogram of styrene reaction mixture (Scheme S1, Eqn. 1)

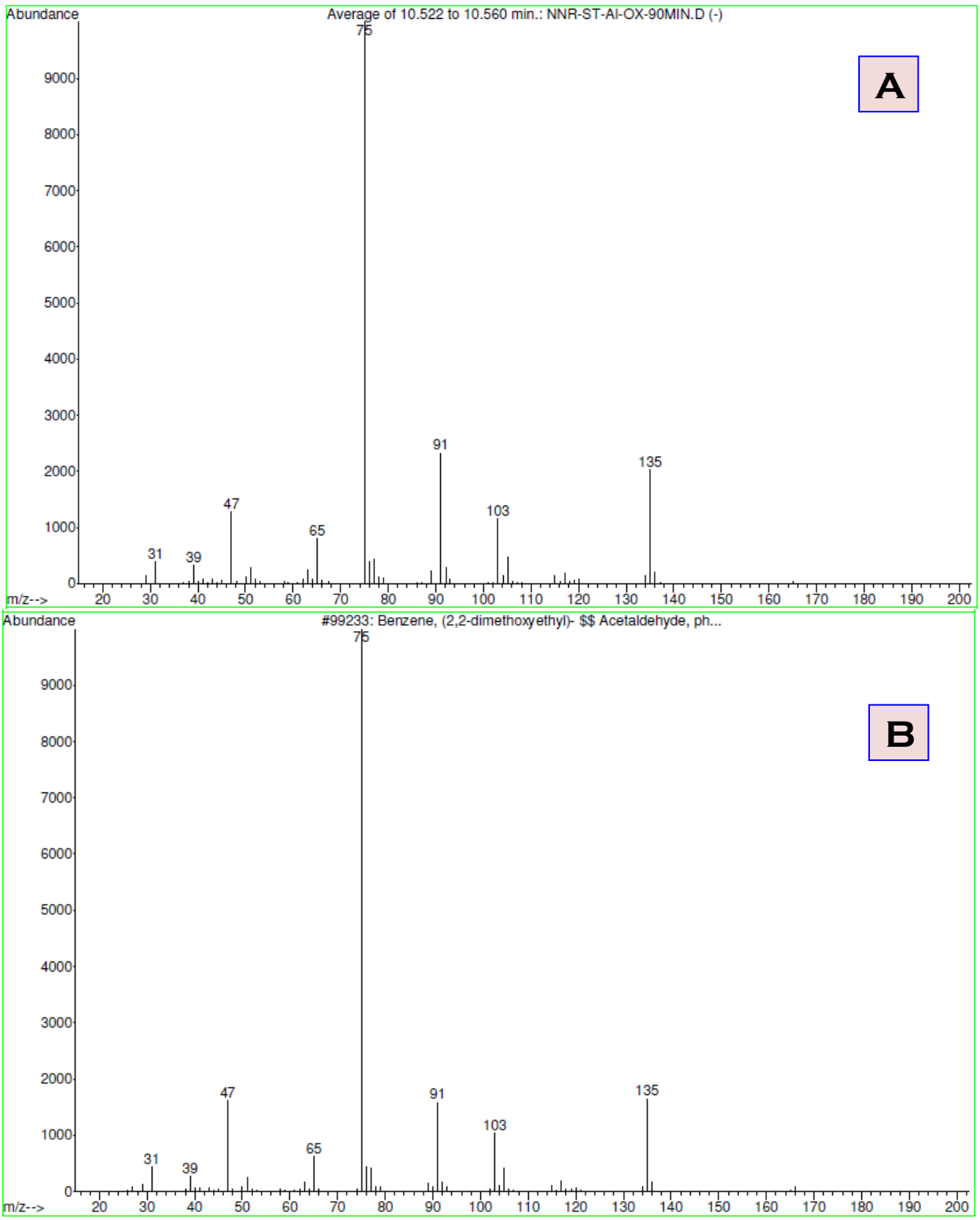

Figure S4. A) EI mass spectrum of peak at t_R = 10.55 min in styrene reaction mixture chromatogram. B) Wiley NIST II Library mass spectrum of (2,2-dimethoxyethyl)benzene (**2a**)

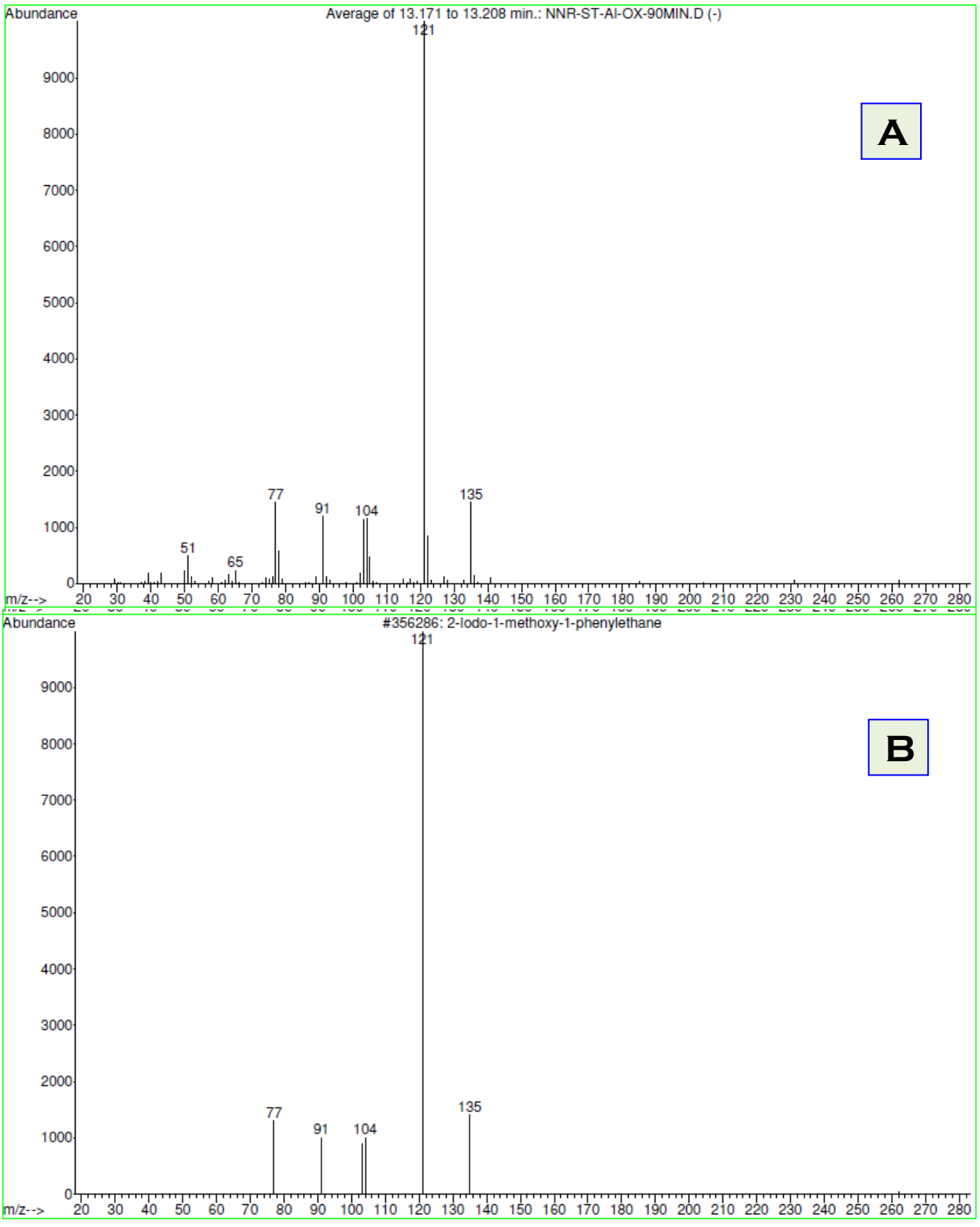

Figure S5. A) EI mass spectrum of peak at t_R = 13.19 min in styrene reaction mixture chromatogram. B) Wiley NIST II Library mass spectrum of 2-iodo-1-methoxy-1-phenylethane (**3a**)

In principle, the both radical and ionic mechanisms can be envisaged for this metal-free acetalization reaction. Recently, Zhang proposed that iodine radical ($I^{\bullet}$) could involves in the iodide ion/*m*-CPBA reagent system catalyzed α-methoxylation of ketones.[3] To confirm

whether our iodide ion/oxone mediated catalytic addition of methanol to alkenes proceeds *via* a radical or an ionic or both mechanisms, we have investigated the metal-free acetalization of styrene in the presence of 2,2,6,6-tetramethylpiperidin-1-oxyl (TEMPO),[4] a radical scavenger, as shown in scheme S1 (Eqn. 2) and obtained the yield of the desired methyl acetal **2a** in 83% yield. This experiment clearly indicating that the reaction did not involve radical mechanism.

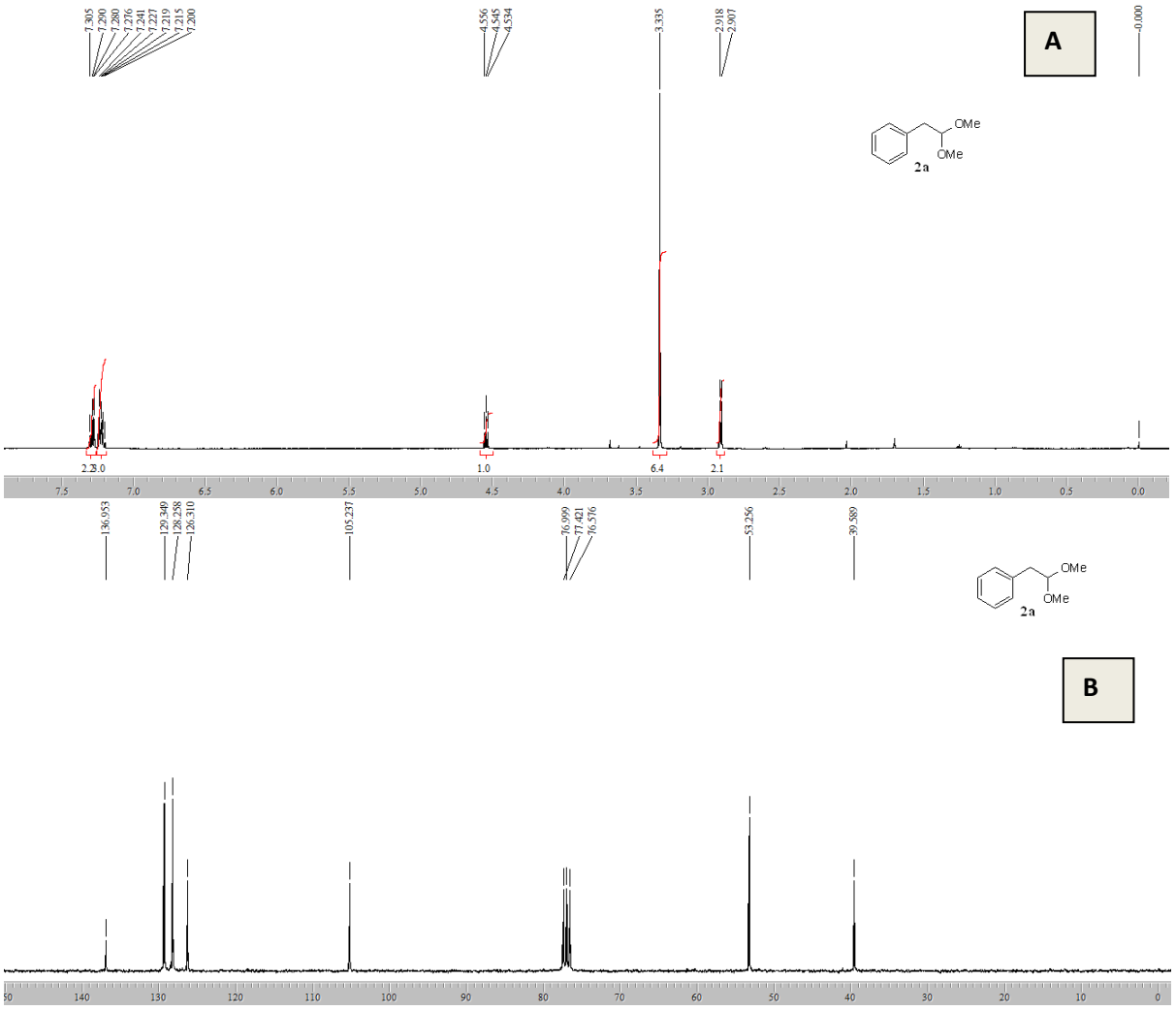

Figure S6. ^{1}H NMR spectrum (A) and ^{13}C NMR spectrum (B) of the product isolated in the styrene reaction (Scheme S1, Eqn. 1).

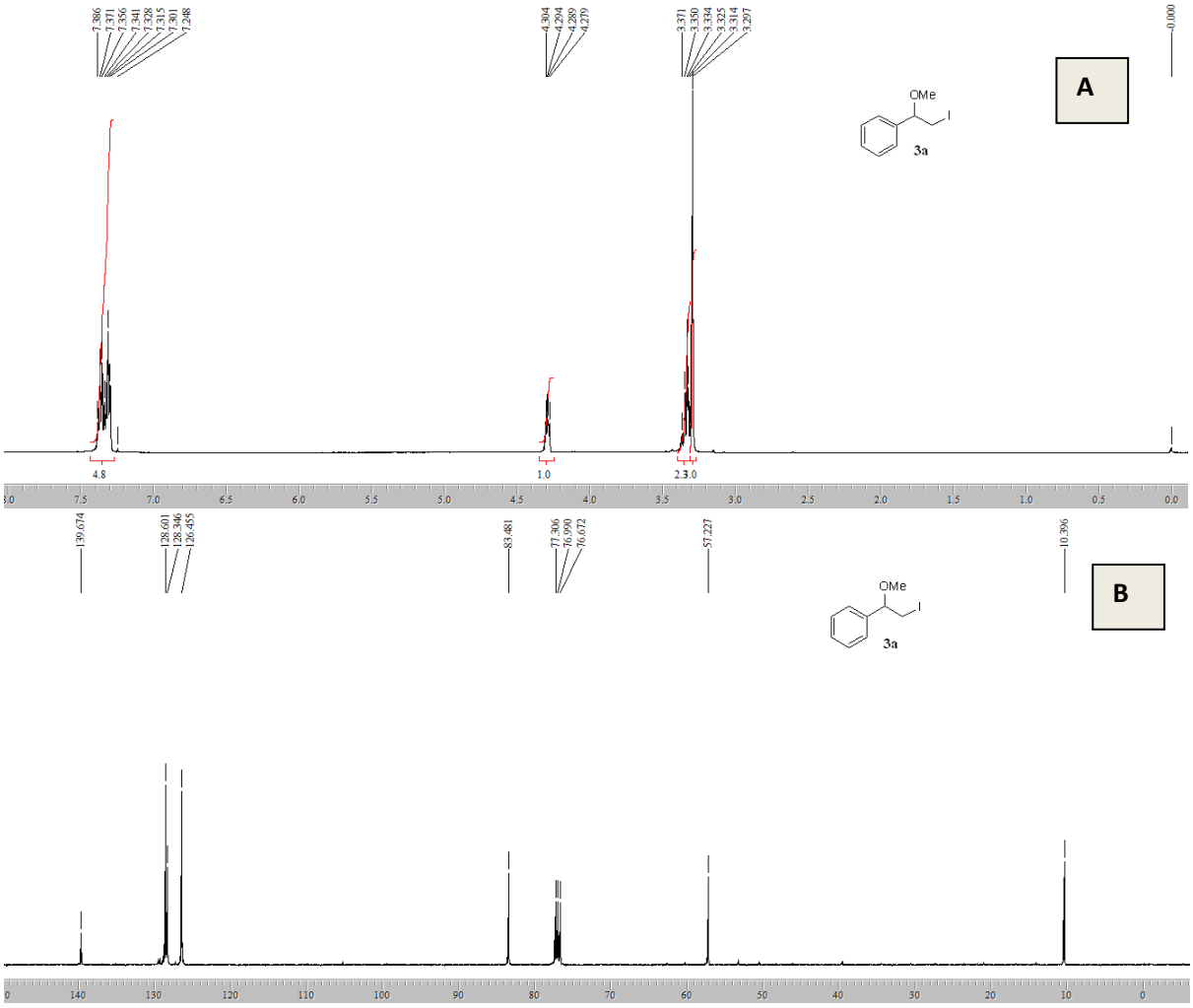

Figure S7. ^{1}H NMR spectrum (A) and ^{13}C NMR spectrum (B) of an intermediate isolated in the styrene reaction (Scheme S1, Eqn. 1).

Next, the intermediacy of **3a** in the conversion of styrene to corresponding acetal **2a** was established based on the experiments shown in Eqn.3 and Eqn.4 (Scheme S1). When the **3a** was subjected to standard conditions, the formation of desired product **2a** was observed in 85% yield (Scheme S1, Eqn. 3). The use of **3a** as pre-catalyst instead of NH_4I also transformed the substrate **1a** efficiently to the desired acetal **2a** (Scheme S1, Eqn. 4). The results of these both reactions (Eqns. 3-4) seems to be a clear indication of co-iodo product (**3**) as a key intermediate for the synthesis of terminal methyl acetals from corresponding aromatic olefins under standard conditions. However, the product **2a** formation could be achieved by the loss of iodine from **3a** followed by the nucleophilic addition of another methanol molecule. In the literature,[5-6] it has been proposed that the co-iodo intermediate can be de-iodinated with the assistance of either bronsted acid sites or basic additives or active electrophilic species generated *in situ*. Therefore, we have carried out few experiments to

gain more information about active species assisted in the de-iodination of **3a** under present reaction conditions (Scheme S1, Eqns. 5-8). The reaction of **3a** in the absence of NH_4I and oxone or oxone alone led to no desired product (Scheme S1, Eqns. 5-6). Next, the reaction was carried out in presence of bronsted acid and observed that the reaction did not occur even after 24 h (Scheme S1, Eqn. 7). But, the formation of product **2a** was observed in the presence of NH_4I and oxone or oxone alone (Scheme S1, Eqns. 3 and 8). These reactions clearly indicating that no bronsted acid or no electrophilic iodine species are responsible for de-iodination and only the oxone is crucial for transforming **3a** to **2a** in our conditions.

2.2. Isotope Labeling Experiment

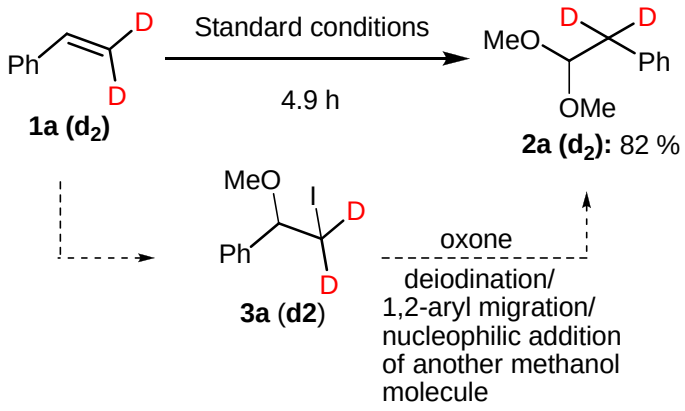

Scheme S2

The earlier control experiments endorsing that the conversion of an aromatic alkene **1** into the corresponding terminal methyl acetal **2** proceeds *via* the formation of co-iodinated intermediate **3**. Moreover, the products of 1,2-disubstituted olefins (Table 1, manuscript, entries 16-17 and 20-21) indicating that the geminal dimethoxylation may proceed *via* de-iodination of intermediate **3** followed by sequential semipinacol type rearrangement and nucleophilic attack of another methanol molecule. To confirm this migration process, we have investigated the reaction of *β,β*-dideuterated styrene using the standard conditions in methanol (Scheme S2) and the product was characterized by NMR spectroscopy.

The proton NMR spectrum of non-deuterated acetal **2a** shows a doublet at 2.91 ppm which corresponds to the benzylic protons (Figure S6A). The proton NMR spectrum of deuterated acetal **2a (d_2)** contains no doublet at 2.91 ppm (Figure S8). Further, the carbon-13 NMR spectrum of non-deuterated acetal **2a** shows peak at 39 ppm (singlet, benzylic carbon) (Figure S6B) whereas, the carbon-13 NMR spectrum of deuterated acetal **2a (d_2)** contains a

low intense multiplet at 39 ppm (multiplet, benzylic carbon) (Figure S9).The NMR analysis of the products **2a** and **2a (d_2)** (obtained from the reaction of styrene and *β,β*-dideuterated styrene, respectively, under standard conditions) indicating that the product **2a (d2)** contains two deuterium atoms at benzylic position. This could be possible only when phenyl group migrates from one carbon to another carbon *via* a transient phenonium ion intermediate **D**.[6] This isotope labelling study unambiguously confirming that the acetalization process proceeds through the rearrangement of aryl group followed by nucleophilic attack of methanol at the carbon atom bearing methoxide group.

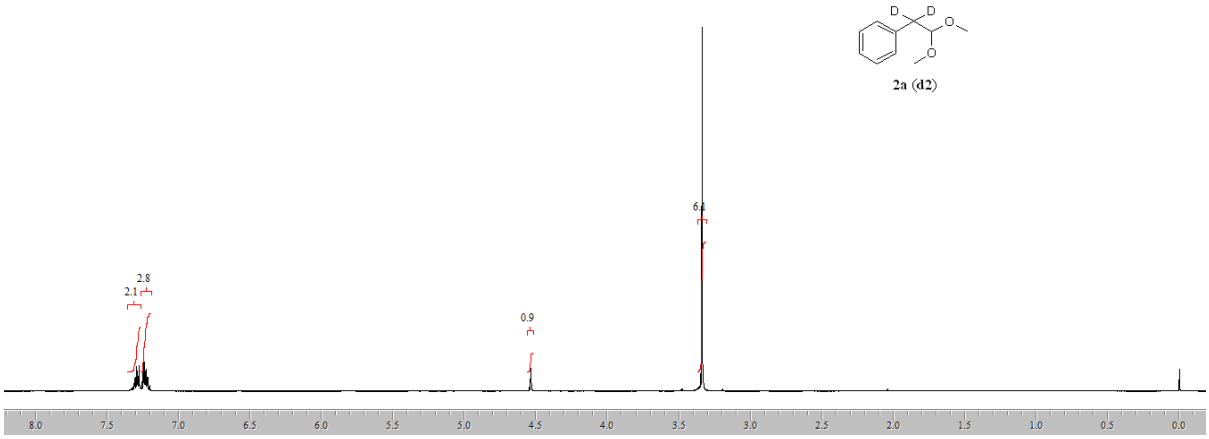

Figure S8. ^{1}H NMR spectrum of deuterated acetal (**2a(d2)**).

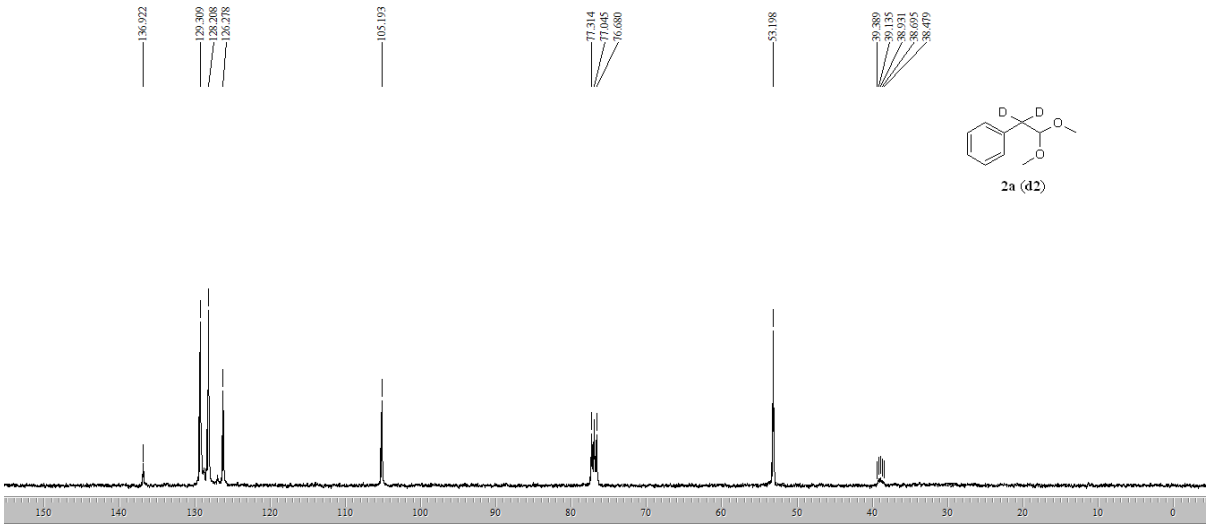

Figure S9. ^{13}C NMR spectrum of deuterated acetal (**2a(d2)**).

2.3. Detection of Reactive Intermediates by High Resolution ESI-MS experiments

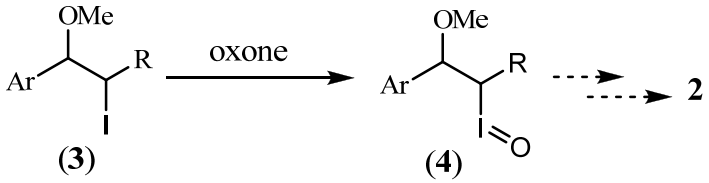

Scheme S3

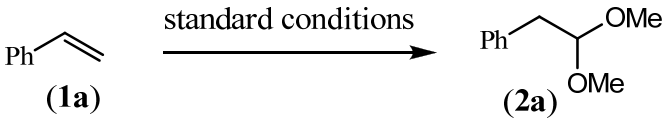

Scheme S4

After confirming the involvement of semipinacol rearrangement in the conversion of vinylarenes to corresponding *anti*-Markovnikov methyl acetals by isotopic study, we were interested in identifying the reactive species, formed *in situ* during the conversion of **1** to **2**, by High Resolution Electrospray Ionization Mass Spectrometry (HRESI-MS) for a thorough understanding of reaction pathway.

The ESI-MS assists in the study of liquid solutions and open up access to the direct investigation of chemical reactions in solution using mass spectrometry.[7] In principle, the ESI-MS provide new insights into the reaction mechanism by detecting and studying not only of reaction substrates and products but even of short-lived reaction intermediates.[8]

In control experiments, it was found that the oxone is crucial for the conversion of co-iodinated intermediate **3** to the desired terminal acetal **2**. In this transformation the oxone may oxidize **3** to hypervalent iodine compound **4** (Scheme S3) that may forms adduct **C** with methanol and undergoes reductive elimination[3] to provide the desired dimethoxylation product *via* a transient phenonium ion, intermediate **D**. Henceforth, we were interested in performing the HRESI-MS experiments on the model reaction of acetalization in order to gain the experimental evidence about the reactive intermediates formed *in situ* under metal-free catalytic conditions.

With a view to understand ESI-MS behaviour of the isolated intermediate **3a** and the product **2a** of styrene acetalization reaction, we have analyzed these two compounds under

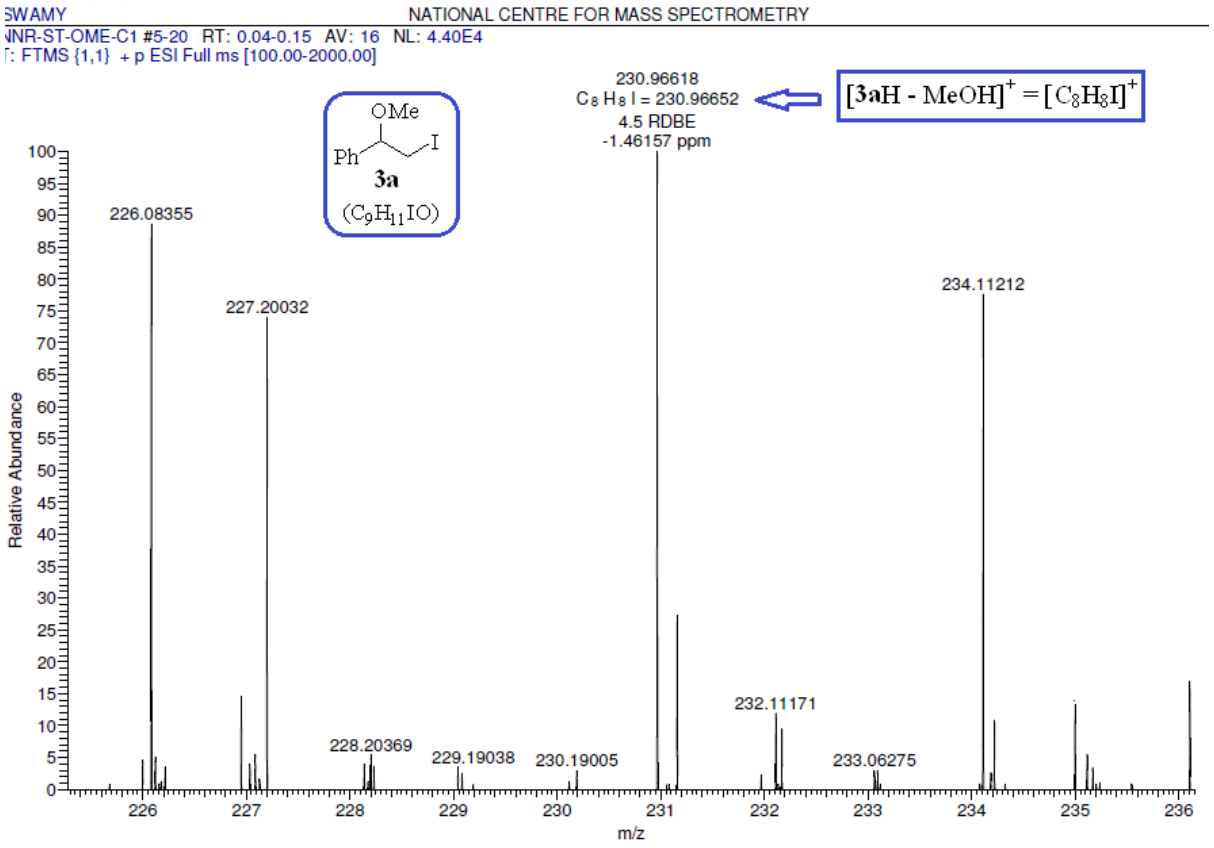

Figure S10. High Resolution ESI-MS spectrum (positive mode) of **3a**.

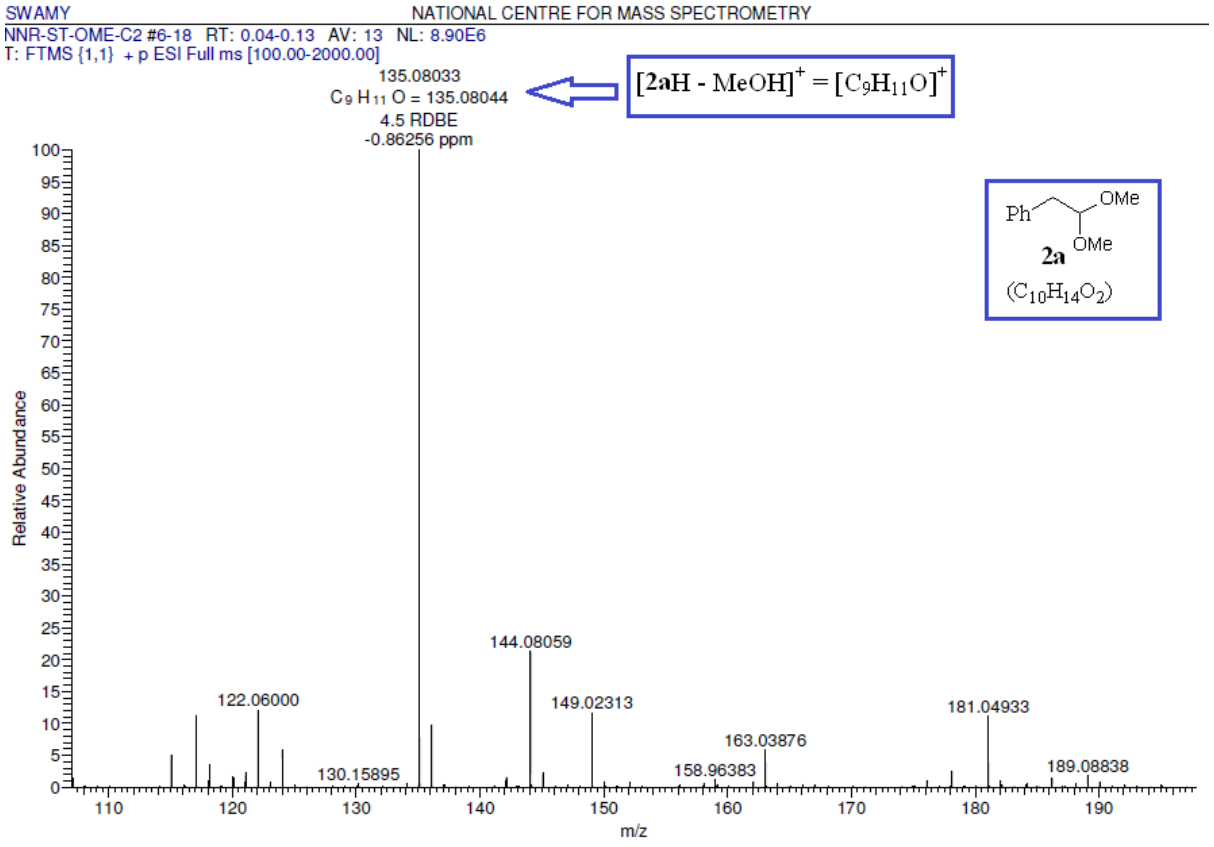

Figure S11. High Resolution ESI-MS spectrum (positive mode) of **2a**.

HRESI-MS conditions before studying the styrene (**1a**) acetalization reaction mixture (Scheme S4). The HRESI mass spectrum (positive mode) of the intermediate **3a** did not show $[M+H]^+$ ion (expected at *m/z* = 262.99328; whose theoretical elemental composition is $C_9H_{12}IO$). But, it showed abundant peak at *m/z* = 230.96618 which corresponds to the ion resulted by loss of methanol from protonated **3a** i.e., $[\mathbf{3a}H - MeOH]^+$, whose calculated *m/z* is 230.96652 and theoretical elemental composition is C_8H_8I (Figure S10). Similarly, the ESI mass spectrum of **2a** showed an abundant peak at *m/z* = 135.08033 that corresponds loss of methanol from protonated molecule i.e., $[\mathbf{2a}H - MeOH]^+$ whose theoretical elemental composition is $C_9H_{11}O$ and *m/z* is 135.08044 (Figure S11). These experiments suggests that the above intermediate/product shows only a loss of methanol peak, but not $[M+H]^+$ under ESI-MS conditions.

Next, the ESI-MS experiments were performed on the styrene acetalization reaction mixture by collecting the sample at different time intervals (zero min, 30 min, 60 min and 150 min) and diluted with two volumes of methanol before introducing into the HRESI source through flow injection (10 μL loop; methanol was used as the mobile phase at a flow rate of 30 μL/min).

The positive ion HRESI mass spectrum of the reaction mixture at 30 min showed predominant peak corresponding to the starting material i.e., styrene (**1a**) whereas the high mass region of the spectrum shows peaks due to reaction intermediates. Hence, the mass spectrum was zoomed out between *m/z* 120 to 245 and 223 to 254, and are shown in Figure S12 and Figure S13, respectively. Since the ESIMS spectrum of isolated product **2a** shown the $[MH - MeOH]^+$ instead of $[M+H]^+$, the ion at *m/z* = 135.08011 in positive ion HRESI mass spectrum at 30 min (Figure S12) is assigned to the product **2a**. A transient phenonium ion intermediate **D**, if stable enough to detect by ESI mass spectrometry, is expected to be detected at *m/z* = 135.08044. Moreover, the accurate mass of intermediate **D** and $[MH – MeOH]^+$ ion from **2a** are essential same. Hence, the contribution of the phenonium ion for the detected peak at *m/z* = 135.08011 cannot be ruled out. Similarly, the ion detected at *m/z* = 230.96590 (Figures S12-S13) is assigned to $[MH – MeOH]^+$ ion of an intermediate **3a**.

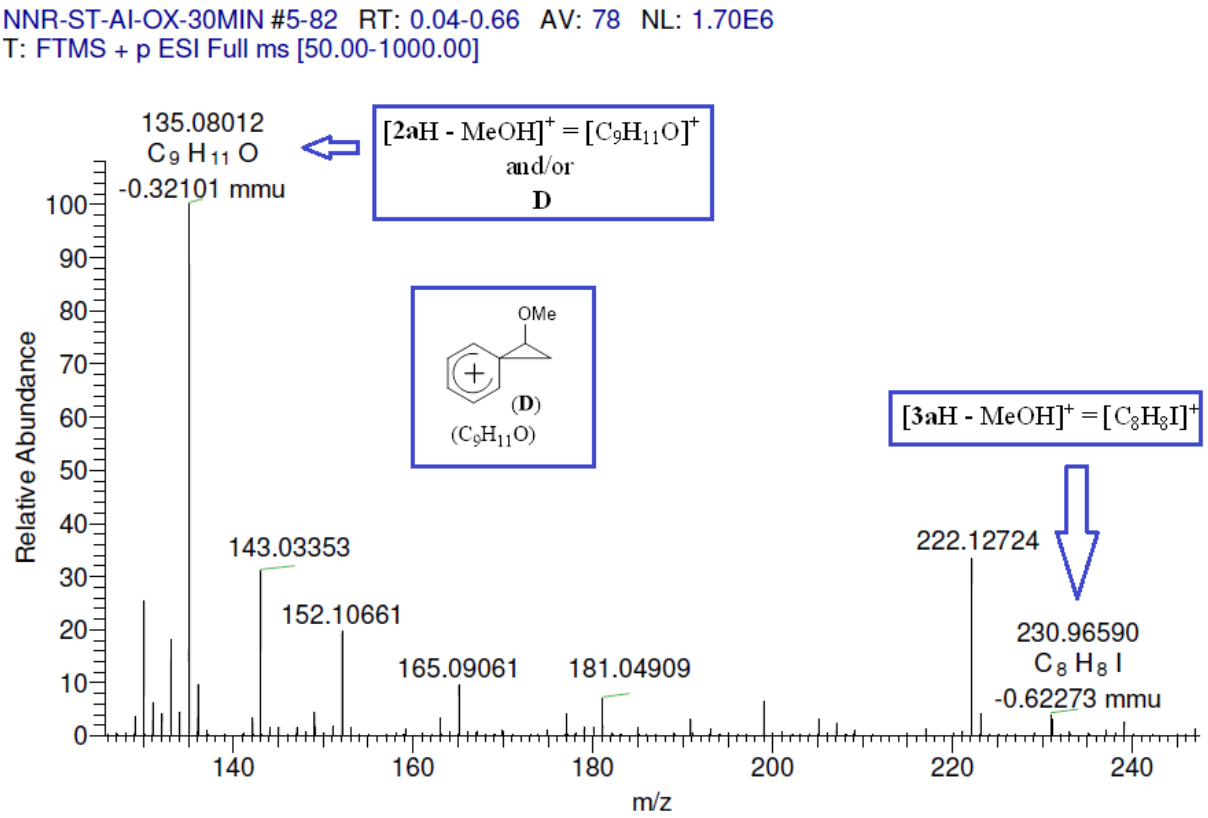

Figure S12. High Resolution ESI-MS spectrum (positive mode) of styrene acetalization reaction mixture (after 30 min, enlarged between *m/z* = 120 and *m/z* = 245).

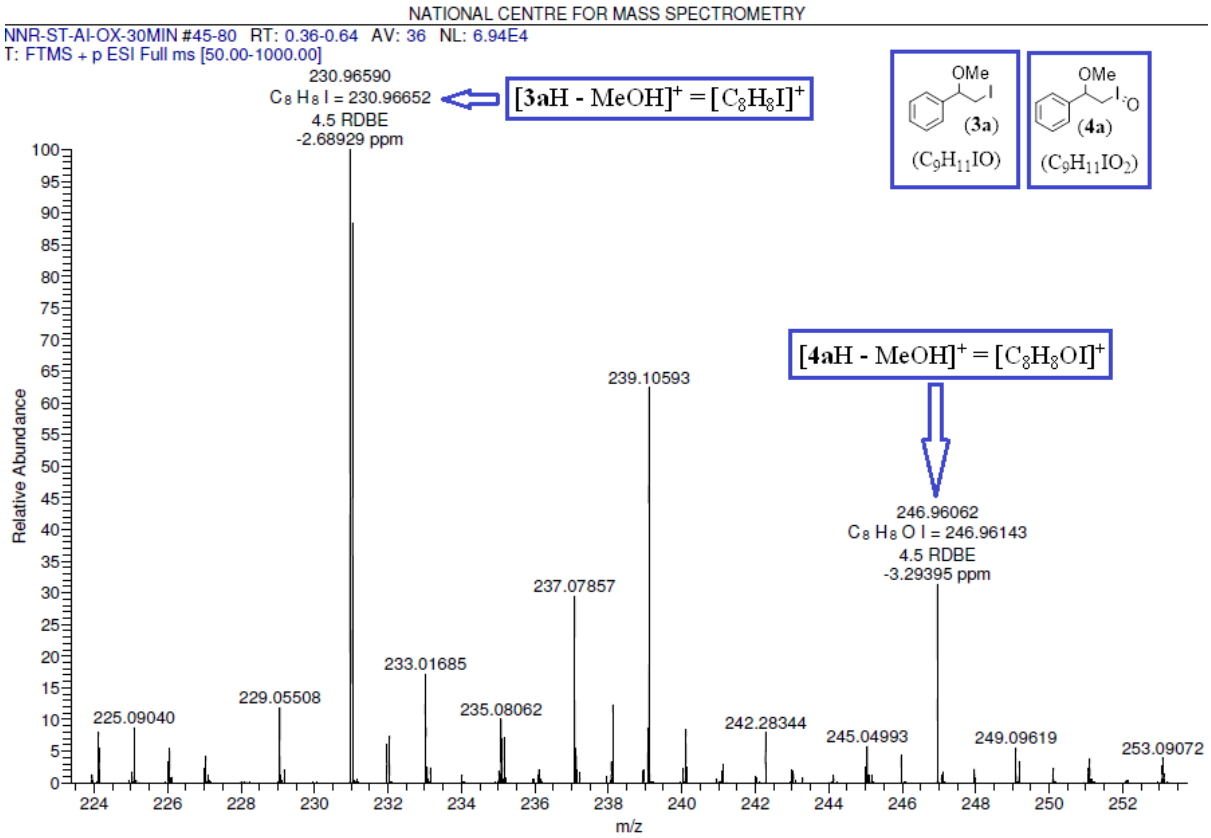

Figure S13. High Resolution ESI-MS (positive mode) spectrum of styrene acetalization reaction mixture (after 30 min, enlarged between *m/z* = 223 and *m/z* = 254).

The spectrum also contains a peak at *m/z* = 246.96062, whose elemental composition found to C_8H_8IO (Figure S13). We have already observed that the ESI-MS of **2a** and **3a** showed $[MH - MeOH]^+$ instead of $[M+H]^+$ ions. Considering the similar behaviour, the intermediate **4a** is expected to form an ion at *m/z* = 246.96143 under ESI-MS conditions. Thus the above detection of *m/z* = 246.96062 with elemental composition C_8H_8IO in the reaction mixture confirms the formation of **4a** *in situ* by the oxidation of **3a**.

These ESI-MS experiments allowed us to detect the hypervalent iodine compound (co-iodo compound **4a**) for the first time, which could be formed *in situ* by the oxidation of isolable intermediate **3a**. This experimental evidence also permits to clear understanding of reaction path in the conversion of intermediate **3** to **2** *via* the de-iodination, thru oxidation of **3** by oxone to **4** followed by reductive elimination,[3] induced rearrangement of aryl group through the formation of transient phenonium ion **D** followed by nucleophilic addition of another methanol molecule at the carbon atom bearing methoxide group, which led to the desired anti-Markovnikov acetal **2**.

2.4. UV-Vis Absorption Spectral Studies

With an intention to identify the active electrophilic iodine species formed by the oxidation of iodide ion by oxone in methanol, we further studied the reaction of NH_4I with oxone under standard conditions in presence and absence of styrene using the UV-Vis spectrophotometer.

The scanning of UV/Vis absorption spectra of the reaction mixture (after stirring for 2 min) of NH_4I and oxone in the absence of styrene indicating the formation of I_3^- (Figure S14B). Upon further stirring (about 20-25 min from oxone addition), the decrease in absorbance at 290 and 358 nm and an increase in absorbance at 444 nm was observed (Figure S14C).

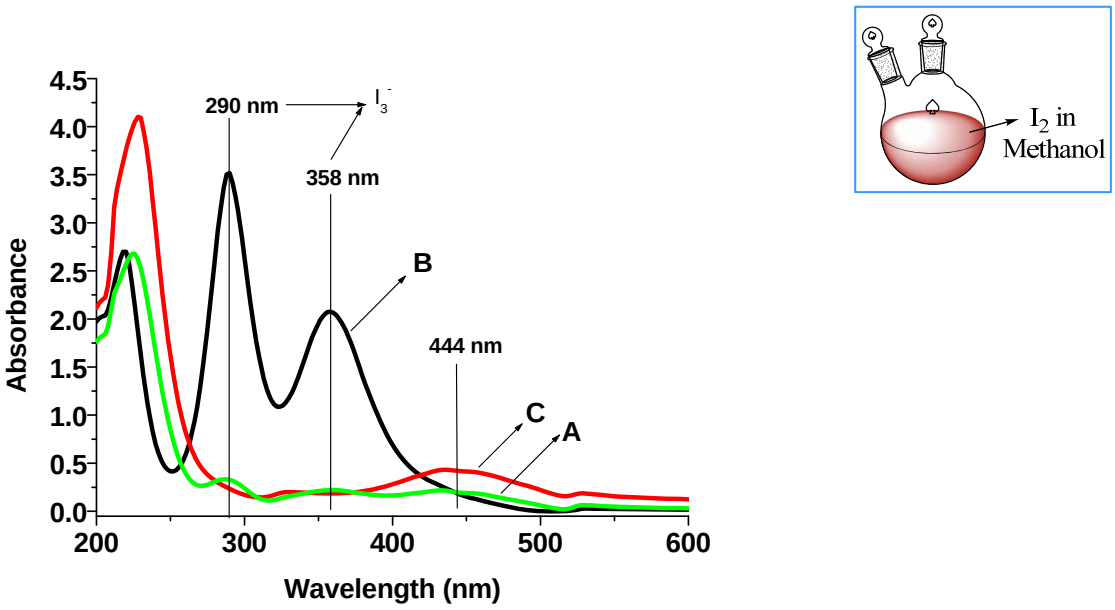

Figure S14. UV-Vis absorption spectrum of (A) I_2 in methanol (peak at 444 nm is the characteristic of I_2, peaks at 290 and 358 nm are due to triiodide impurity), (B) reaction of NH_4I and oxone in the absence of styrene under standard conditions after 2 min and (C) after 20 min.

It has been reported in the literature that the oxidation of iodide ion by oxidant generates transient HOI species, which can be readily converted into molecular iodine under high acidic conditions, by reacting with unreacted iodide ions (Scheme S5, Eqn. 1) or by disproportionation (Scheme S5, Eqn. 2), in the absence of oxidizable organic compounds or other inorganic species.[9] Then, the I_2 reacts rapidly with unreacted I^- to form I_3^-. The above experiment clearly indicating that the oxone converts I^- to I_3^- and I_3^- to I_2 in our conditions. Based on the literature report, we expected that the triiodide ion may be formed according to the Eqns 1-3 (Scheme S5). Moreover, G. Lente and co-workers proposed that the oxone converts I_2 to IO_3^- *via* formation of HOI (Scheme S5, Eq. 4).[10]

$$HOI + I^- \xrightarrow[H^+]{\text{fast}} I_2 + H_2O \quad \text{---------} \quad (1)$$

$$HOI \xrightarrow[H^+]{\text{disproportionation}} I_2 \quad \text{---------} \quad (2)$$

$$I_2 + I^- \xrightarrow[H^+]{\text{fast}} I_3^- \quad \text{---------} \quad (3)$$

$$I_2 \text{ or } I_3^- \xrightarrow[(\textit{via}\ HOI)]{\text{oxone}} HIO_3 \quad \text{---------} \quad (4)$$

Scheme S5

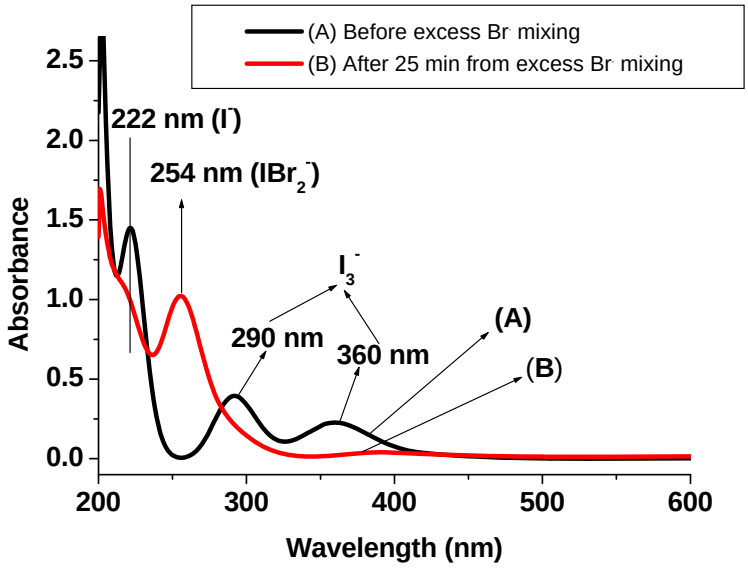

Figure S15. (A) UV-Vis spectrum of reaction of NH_4I (0.2 mmol) and oxone (1 mmol) in 5 mL of methanol at 30 ^oC (before excess bromide ion mixing). (B) UV-Vis spectrum of reaction of NH_4I (0.2 mmol) and oxone (1 mmol) in presence of excess Br^- in 5 mL of methanol at 30 ^oC (after 25 min from bromide ion mixing)

In order to confirm the *in situ* generation of HOI by the oxidation of I^-, the oxidation of iodide ion in presence of excess bromide ion was studied at different time intervals using UV-Vis spectrophotometry. The scanning of UV/Vis absorption spectrum of the reaction mixture of NH_4I and oxone in the absence of excess Br^- indicating the formation of I_3^- (Figure S15), which is consistence with our earlier experiment. When the excess bromide ion is added to the above reaction mixture and recorded the absorption spectra after 25 min, disappearance of I_3^- and I^- ions and the appearance of new absorption peak at 254 nm was observed. The peak at 254 nm was assigned to IBr_2^- based on the literature report.[9] The IBr_2^- can be formed according to the Eqns 1-2 (Scheme S6) at low P^H values. This UV-Vis study of reaction of NH_4I and oxone under standard conditions in presence of excess Br^- unambiguously confirming that the oxidation of iodide ion generates HOI species *in situ* which are highly unstable under acidic conditions.

$$HOI + Br^- + H^+ \rightleftharpoons IBr + H_2O \qquad K = 4.2 \times 10^6\ M^{-2} \qquad \text{-------} (1)$$

$$IBr + Br^- \rightleftharpoons IBr_2^- \qquad K = 286\ M^{-1} \qquad \text{-------} (2)$$

Scheme S6

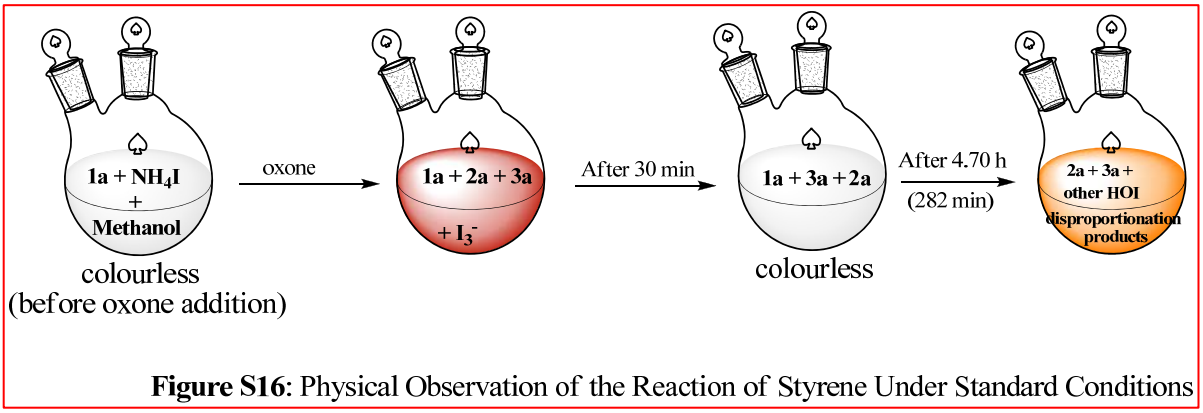

Figure S16: Physical Observation of the Reaction of Styrene Under Standard Conditions

After confirming the *in situ* generation of transient HOI species in our conditions, the physical appearance the acetalization reaction was observed during the progress of the reaction. In the absence of oxone, the reaction mixture, for example styrene acetalization reaction (Figure S16), was in colorless and when the oxone was added to the above solution, it turns instantaneously into reddish brown color. This color retains up to 20 min and decreasing its intensity with increasing the reaction time. After 30 min, the reaction mixture becomes colourless and retains until 280 min, and the solution starts acquiring yellowish orange color before 15 min of completion of the reaction. This physical observation and the above UV-Vis absorption spectrum of the reaction of NH_4I and oxone in the absence of styrene suggesting that initially the color of the reaction mixture due to the formation of I_3^- according to Eqns. 1-3 (Scheme S5) and the decrease in intensity of I_3^- upon stirring possibly due to its oxidation to HOI *via* formation of I_2 by oxone. Although the oxidation of iodide ion by oxone led to the formation of I_3^- and I_2, which could not be the active catalytic species because during the progress of the reaction between 30 min to 282 min (the total reaction time is 297 min), the solution did not acquires any color and appears in the colorless form. If any trace amounts of molecular iodine or triiodide ions regenerated during the catalytic conversion of vinylarenes to acetals, the reaction mixture should attain reddish brown color or any other color. Therefore, the active catalytic species may be the transient HOI species, formed by the oxidation of iodide ion and the triiodide ion, and the color after completion of reaction may be due to the presence of products formed by the disproportionation of transient HOI under acidic conditions in the absence of oxidizable alkene moieties.

When the styrene acetalization reaction (at different time intervals) was studied using the UV-Vis spectrophotometer (*see* Figure S17), the absorption spectrum at 2 min contains one broad absorption peak with few shoulder peaks and a weak absorption peak at 360 nm. The peak at 360 nm is one of the characteristic peaks of triiodide ion (*see* Figure S14) and the

other characteristic peak at 290 nm was over shaded by the broad absorption peak due to the styrene reaction intermediates and products. The peak at 360 nm clearly indicating that the reddish brown color of the solution is due to formation of triiodide ion and the peak was no longer visible due to its oxidation in presence of oxone, which is consistent with the results of earlier experiments (Figures S14-S17). Further, the spectrum also contains a peak at 278 nm and its intensity decreased during the progress of the reaction (Figure S17). It is well known that the HOI species shows characteristic absorption at 278 nm.[11] However, no I_3^- or I_2 absorption peaks were observed in 30 min and 287 min spectra and the absorption peak at 278 nm is appeared in the 30 min spectrum possibly due to its regeneration in the catalytic cycle and is disappeared in 287 min spectrum maybe due to its disproportionation in the absence of oxidizable alkene moieties under acidic conditions.

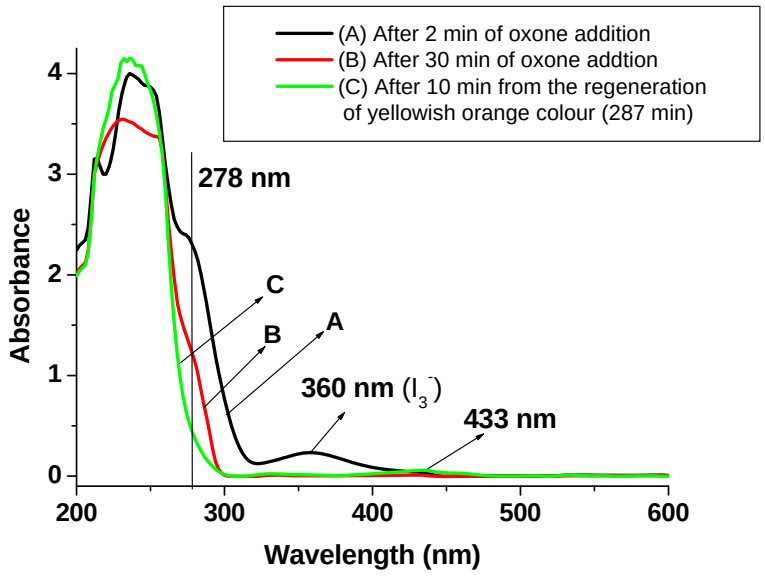

Figure S17. Spectrophotometric behaviour of styrene acetalization reaction under standard conditions at different time intervals

These UV/Vis absorption studies suggesting that the HOI species are the active catalytic species in the iodide salt/oxone mediated catalytic addition of methanol to alkenes. Moreover, the mass spectrometry experiments also signifying that the de-iodination of co-iodo intermediate **3**, *via* its oxidation to trivalent iodine species **4** followed by reductive elimination, led to the regeneration of HOI species. It could be concluded from the both spectrometric studies (Mass and UV/Vis) that the oxidation of iodide ion by oxone generates hypoiodous acid which competitively reacts with electron rich alkene moiety and unreacted iodide ion to form co-iodo intermediated **3** and triiodide ion, respectively. The I_3^- reconverted

into HOI and the intermediate **3** further oxidized to hypervalent species **4** in presence of oxone. The HOI species regenerated from the reductive elimination of **4** and from the oxidation of triiodide ion continues the catalytic cycle until complete consumption of the substrate.

3. Spectroscopic data of products:

4-methyl-1-(2,2-dimethoxyethyl)benzene (**2b**)[2]

^{1}H NMR (500 MHz, $CDCl_3$): δ (ppm) = 7.18-7.02 (m, 4 H), 4.52 (t, J = 5.49, Hz, 1 H), 3.32 (s, 6 H), 2.87 (d, J = 5.49 Hz, 2 H), 2.31 (s, 3 H).

^{13}C NMR (125 MHz, $CDCl_3$): δ (ppm) = 135.72, 133.81, 129.18, 128.92, 105.30, 53.14, 39.08, 20.94.

3-methyl-1-(2,2-dimethoxyethyl)benzene (**2c**)[2]

^{1}H NMR (500 MHz, $CDCl_3$): δ (ppm) = 7.29-7.13 (m, 4 H), 4.54 (t, J = 5.66, Hz, 1 H), 3.33 (s, 6 H), 2.88 (d, J = 5.66 Hz, 2 H), 2.33 (s, 3 H).

^{13}C NMR (125 MHz, $CDCl_3$): δ (ppm) = 137.78, 136.87, 130.13, 128.15, 127.07, 126.33, 105.27, 53.19, 39.49, 21.35.

4-*tert*-butyl-1-(2,2-dimethoxyethyl)benzene (**2d**)

^{1}H NMR (500 MHz, $CDCl_3$): δ (ppm) = 7.31 (d, J = 8.39 Hz, 2 H), 7.17 (d, J = 8.39 Hz, 2 H), 4.55 (t, J = 5.64, Hz, 1 H), 3.34 (s, 6 H), 2.88 (d, J = 5.64 Hz, 2 H), 1.30 (s, 9 H).

^{13}C NMR (125 MHz, $CDCl_3$): δ (ppm) = 149.03, 133.86, 128.96, 125.18, 105.15, 53.09, 38.91, 34.33, 31.33.

HRMS-EI: *m/z* $[MH - MeOH]^+$ calcd for $C_{13}H_{19}O$: 191.14359; found: 191.14300.

1-(2,2-dimethoxyethyl)-4-methoxybenzene (**2e**)[2]

^{1}H NMR (500 MHz, $CDCl_3$): δ (ppm) = 7.15 (d, J = 8.39 Hz, 2 H), 6.83 (d, J = 8.39 Hz, 2 H), 4.49 (t, J = 5.64, Hz, 1 H), 3.78 (s, 3 H), 3.33 (s, 6 H), 2.85 (d, J = 5.64 Hz, 2 H).

^{13}C NMR (125 MHz, $CDCl_3$): δ (ppm) = 158.08, 130.27, 130.18, 128.96, 113.91, 113.64, 105.42, 55.10, 53.25, 38.64.

1-(2,2-dimethoxyethyl)-2-methoxybenzene (**2f**)[2]

^{1}H NMR (500 MHz, $CDCl_3$): δ (ppm) = 7.24-7.17 (m, 2 H), 6.93-6.81 (m, 2 H), 4.64 (t, J = 5.79 Hz, 1 H), 3.82 (s, 3 H), 3.32 (s, 6 H), 2.94 (d, J = 5.79 Hz, 2 H).

^{13}C NMR (100 MHz, $CDCl_3$): δ (ppm) = 157.51, 131.20, 127.65, 125.40, 120.38, 110.16, 103.89, 55.25, 53.14, 34.14.

1-(2,2-dimethoxyethyl)-3-nitrobenzene (**2g**)[2]

^{1}H NMR (500 MHz, $CDCl_3$): δ (ppm) = 8.11 (s, 1 H), 8.09 (d, J = 8.08 Hz, 1 H), 7.58 (d, J = 7.62 Hz, 1 H), 7.46 (t, J = 7.78 Hz, 1 H), 4.55 (t, J = 5.49 Hz, 1 H), 3.36 (s, 6 H), 3.02 (d, J = 5.49 Hz, 2 H).

^{13}C NMR (125 MHz, $CDCl_3$): δ (ppm) = 148.18, 138.90, 135.84, 129.05, 124.35, 121.54,

104.50, 53.61, 39.18.

1-(1,2-dimethoxyethyl)-3-nitrobenzene (**2g'**)

^{1}H NMR (500 MHz, $CDCl_3$): δ (ppm) = 8.21 (s, 1 H), 8.18 (d, J = 8.08 Hz, 1 H), 7.70 (d, J = 7.62 Hz, 1 H), 7.56 (t, J = 7.78 Hz, 1 H), 4.49 (dd, J = 7.12, 4.12 Hz, 1 H), 3.61 (dd, J = 10.37, 7.12 Hz, 1 H), 3.48 (dd, J = 10.22, 4.12 Hz, 1 H), 3.39 (s, 3 H), 3.34 (s, 3 H).

^{13}C NMR (75 MHz, $CDCl_3$): δ (ppm) = 148.32, 141.40, 133.00, 129.38, 122.93, 121.85, 81.85, 76.29, 59.26, 57.35.

HRMS-EI: *m/z* $[MH - MeOH]^+$ calcd for $C_9H_{10}NO_3$: 180.06607; found: 180.06600.

1-(2,2-dimethoxyethyl)-4-trifluoromethylbenzene (2h)[12]

^{1}H NMR (500 MHz, $CDCl_3$): δ (ppm) = 7.54 (d, J = 8.08 Hz, 2 H), 7.35 (d, J = 8.08 Hz, 2 H), 4.53 (t, J = 5.64 Hz, 1 H), 3.34 (s, 6 H), 2.97 (d, J = 5.64 Hz, 2 H).

^{13}C NMR (75 MHz, $CDCl_3$): δ (ppm) = 141.08, 129.76, 125.10, 104.78, 53.43, 39.45.

1-(2,2-dimethoxyethyl)-4-fluorobenzene (**2i**)[2]

^{1}H NMR (500 MHz, $CDCl_3$): δ (ppm) = 7.22-7.16 (m, 2 H), 7.00-6.94 (m, 2 H), 4.48 (t, J = 5.64 Hz, 1 H), 3.33 (s, 6 H), 2.88 (d, J = 5.49 Hz, 2 H).

^{13}C NMR (125 MHz, $CDCl_3$): δ (ppm) = 162.56, 160.62, 132.61, 132.59, 130.84, 130.77, 115.51, 114.93, 105.23, 53.40, 38.79.

1-(2,2-dimethoxyethyl)-3-fluorobenzene (**2j**)

^{1}H NMR (500 MHz, $CDCl_3$): δ (ppm) = 7.28-7.20 (m, 1 H), 7.00 (d, J = 7.78 Hz, 1 H), 6.98-6.94 (m, 1 H), 6.93-6.87 (m, 1 H), 4.52 (t, J = 5.64 Hz, 1 H), 3.34 (s, 6 H), 2.90 (d, J = 5.64 Hz, 2 H).

^{13}C NMR (75 MHz, $CDCl_3$): δ (ppm) = 164.36, 161.12, 139.53, 139.43, 129.65, 129.54, 125.06, 116.40, 116.12, 113.36, 113.09, 104.91, 53.35, 39.34.

HRMS-EI: *m/z* $[MH - MeOH]^+$ calcd for $C_9H_{10}FO$: 153.07157; found: 153.07235.

1-chloro-4-(2,2-dimethoxyethyl)benzene (**2k**)[2]

^{1}H NMR (500 MHz, $CDCl_3$): δ (ppm) = 7.25 (d, J = 8.39 Hz, 2 H), 7.16 (d, J = 8.39 Hz, 2 H), 4.49 (t, J = 5.64 Hz, 1 H), 3.33 (s, 6 H), 2.87 (d, J = 5.64 Hz, 2 H).

^{13}C NMR (75 MHz, $CDCl_3$): δ (ppm) = 135.39, 132.17, 130.75, 128.35, 105.01, 53.41, 38.96.

1-chloro-3-(2,2-dimethoxyethyl)benzene (**2l**)[6]

^{1}H NMR (500 MHz, $CDCl_3$): δ (ppm) = 7.25-7.17 (m, 3 H), 7.13-7.09 (m, 1 H), 4.51 (t, J = 5.64 Hz, 1 H), 3.33 (s, 6 H), 2.88 (d, J = 5.64 Hz, 2 H).

^{13}C NMR (75 MHz, $CDCl_3$): δ (ppm) = 138.95, 133.94, 129.46, 129.44, 127.60, 126.51, 104.83, 53.35, 39.23.

1-bromo-4-(2,2-dimethoxyethyl)benzene (**2m**)[13]

^{1}H NMR (500 MHz, $CDCl_3$): δ (ppm) = 7.41 (d, J = 8.30 Hz, 2 H), 7.11 (d, J = 8.30 Hz, 2 H), 4.48 (t, J = 5.47 Hz, 1 H), 3.33 (s, 6 H), 2.86 (d, J = 5.47 Hz, 2 H).

^{13}C NMR (125 MHz, $CDCl_3$): δ (ppm) = 135.89, 131.28, 131.14, 120.24, 104.91, 53.40, 39.00.

1-bromo-3-(2,2-dimethoxyethyl)benzene (**2n**)

^{1}H NMR (300 MHz, $CDCl_3$): δ (ppm) = 7.39 (s, 1 H), 7.37-7.30 (m, 1 H), 7.27-7.10 (m, 2 H), 4.50 (t, J = 5.66 Hz, 1 H), 3.33 (s, 6 H), 2.86 (d, J = 5.66 Hz, 2 H).

^{13}C NMR (75 MHz, $CDCl_3$): δ (ppm) = 139.22, 132.33, 129.71, 129.40, 128.04, 122.20, 104.77, 53.32, 39.16.

HRMS-EI: *m/z* $[MH - MeOH]^+$ calcd for $C_9H_{10}BrO$: 212.99150; found: 212.99140.

2-(2,2-dimethoxyethyl)naphthalene (2o)[2]

^{1}H NMR (300 MHz, $CDCl_3$): δ (ppm) = 7.93-7.63 (m, 4 H), 7.55-7.33 (m, 3 H), 4.63 (t, J = 5.47 Hz, 1 H), 3.35 (s, 6 H), 3.08 (d, J = 5.47 Hz, 2 H).

^{13}C NMR (75 MHz, $CDCl_3$): δ (ppm) = 134.53, 133.46, 132.17, 127.84, 127.77, 127.73, 127.49, 126.09, 125.80, 125.29, 105.33, 53.33, 39.81.

(1,1-dimethoxypropan-2-yl)benzene (2p)[2]

^{1}H NMR (500 MHz, $CDCl_3$): δ (ppm) = 7.34-7.26 (m, 2 H), 7.26-7.16 (m, 3 H), 4.36 (d, J = 6.86 Hz, 1 H), 3.35 (s, 3 H), 3.22 (s, 3 H), 3.00 (m, 1 H), 1.27 (d, J = 7.17 Hz, 3 H).

^{13}C NMR (75 MHz, $CDCl_3$): δ (ppm) = 143.00, 128.16, 127.87, 126.26, 108.56, 54.39, 53.96, 42.89, 16.74.

3,3-dimethoxy-2-phenylpropan-1-ol (2q)

^{1}H NMR (500 MHz, $CDCl_3$): δ (ppm) = 7.38-7.29 (m, 2 H), 7.28-7.18 (m, 3 H), 4.66 (d, J = 7.17 Hz, 1 H), 4.02-3.94 (m, 1 H), 3.77-3.71 (m, 1 H), 3.44 (s, 3 H), 3.25 (s, 3 H), 3.20-3.11 (m, 1 H), 2.75 (brs, 1 H).

^{13}C NMR (75 MHz, $CDCl_3$): δ (ppm) = 138.36, 128.52, 128.39, 126.99, 107.53, 64.30, 55.20, 53.53, 50.58.

HRMS-ESI: *m/z* $[MH - MeOH]^+$ calcd for $C_{10}H_{13}O_2$: 165.09101; found: 165.09078.

1,1-dimethoxy-2,2-diphenylacetaldehyde acetal (2t)[14]

^{1}H NMR (500 MHz, $CDCl_3$): δ (ppm) = 7.27-7.13 (m, 8 H), 7.12-7.03 (m, 2 H), 4.90 (d, J = 7.78 Hz, 1 H), 4.14 (d, J = 7.78 Hz, 1 H), 3.20 (s, 6 H).

^{13}C NMR (75 MHz, $CDCl_3$): δ (ppm) = 141.03, 128.61, 128.25, 126.34, 106.39, 54.47, 53.92.

1,2-diphenyl-1,2-dimethoxyethane (2t')[14]

^{1}H NMR (500 MHz, $CDCl_3$): δ (ppm) = 7.33-7.25 (m, 6 H), 7.21-7.13 (m, 4 H), 4.30 (s, 2 H), 3.15 (s, 6 H).

^{13}C NMR (75 MHz, $CDCl_3$): δ (ppm) = 138.42, 127.99, 127.73, 127.58, 86.88, 57.09.

(2,3-dimethoxypropyl)benzene (2v')

^{1}H NMR (500 MHz, $CDCl_3$): δ (ppm) = 7.32-7.25 (m, 2 H), 7.24-7.17 (m, 2 H), 3.57-3.49 (m, 1 H), 3.42-3.37 (m, 1 H), 3.38 (s, 3 H), 3.36-3.28 (m, 1 H), 3.34 (s, 3 H), 2.90-2.76 (m, 2 H).

^{13}C NMR (125 MHz, $CDCl_3$): δ (ppm) = 138.35, 129.30, 128.19, 126.07, 81.17, 73.28, 59.03, 57.46, 37.18.

HRMS-EI: *m/z* $[MH - MeOH]^+$ calcd for $C_{10}H_{13}O$: 149.09664; found: 149.09601.

1,2-dimethoxydodecane (2w')

^{1}H NMR (300 MHz, $CDCl_3$): δ (ppm) = 3.52-3.35 (m, 9 H), 1.47-1.19 (m, 18 H), 0.88 (t, J = 6.04 Hz, 3 H).

^{13}C NMR (125 MHz, $CDCl_3$): δ (ppm) = 80.05, 74.74, 59.11, 57.28, 31.86, 31.13, 29.75, 29.55, 29.28, 25.33, 22.63, 14.04.

HRMS-EI: *m/z* $[MH - MeOH]^+$ calcd for $C_{13}H_{27}O$: 199.20619; found: 199.20600.

4. Copies of ^{1}H and ^{13}C NMR spectra:

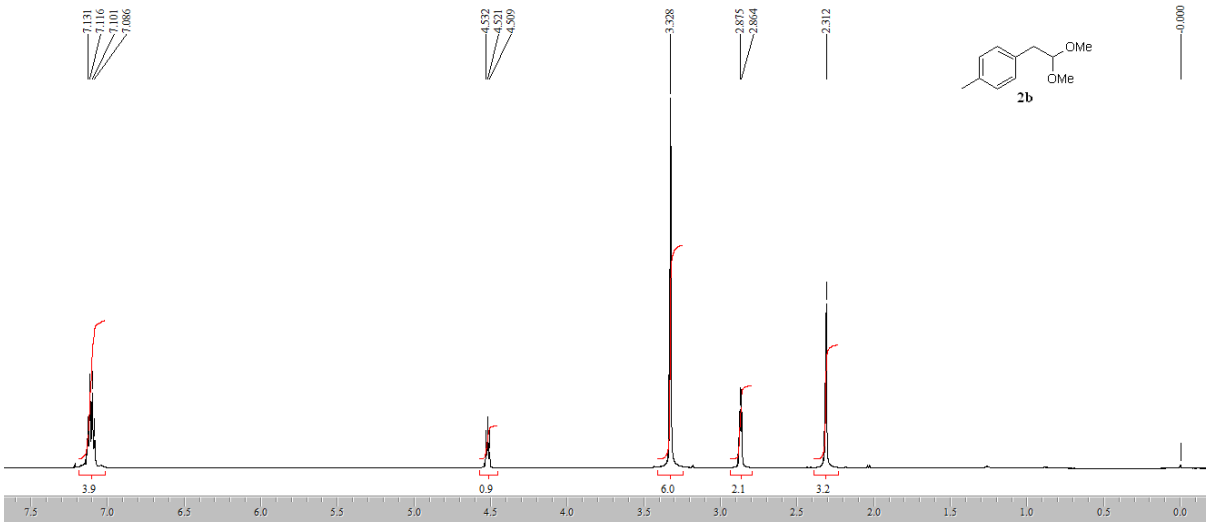

Figure S18

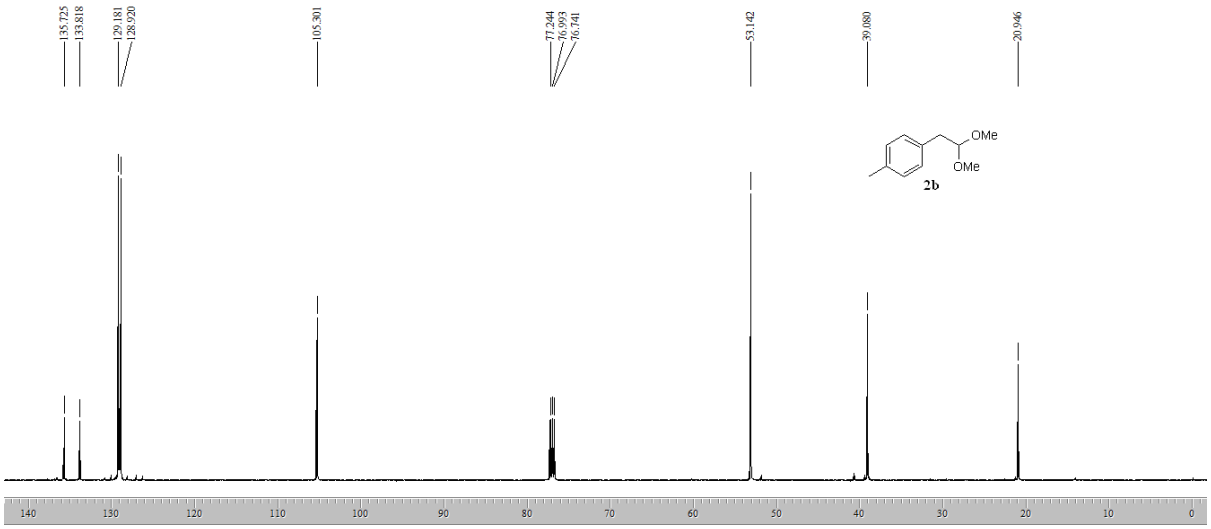

Figure S19

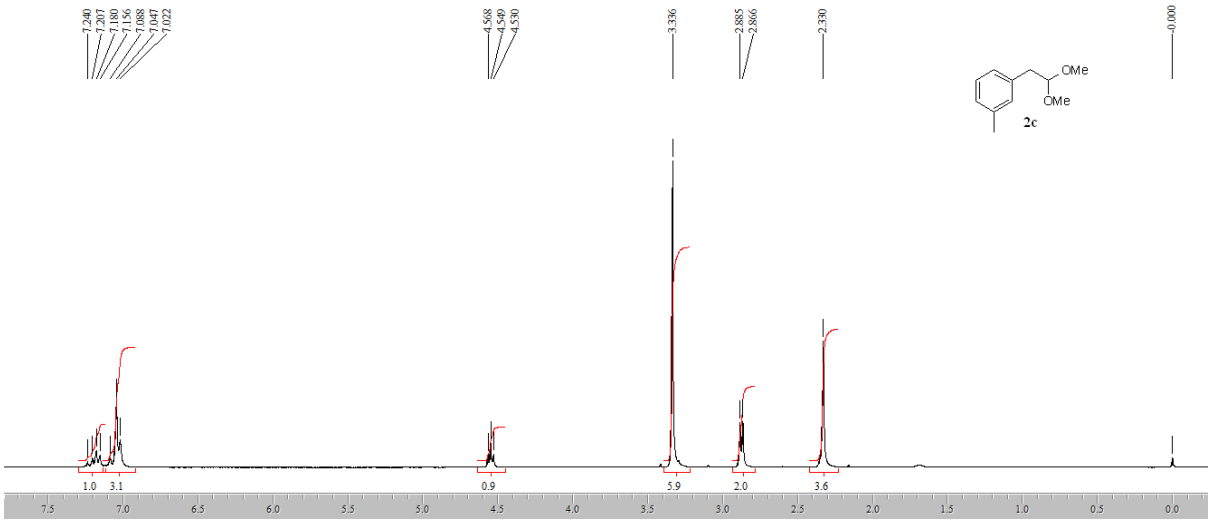

Figure S20

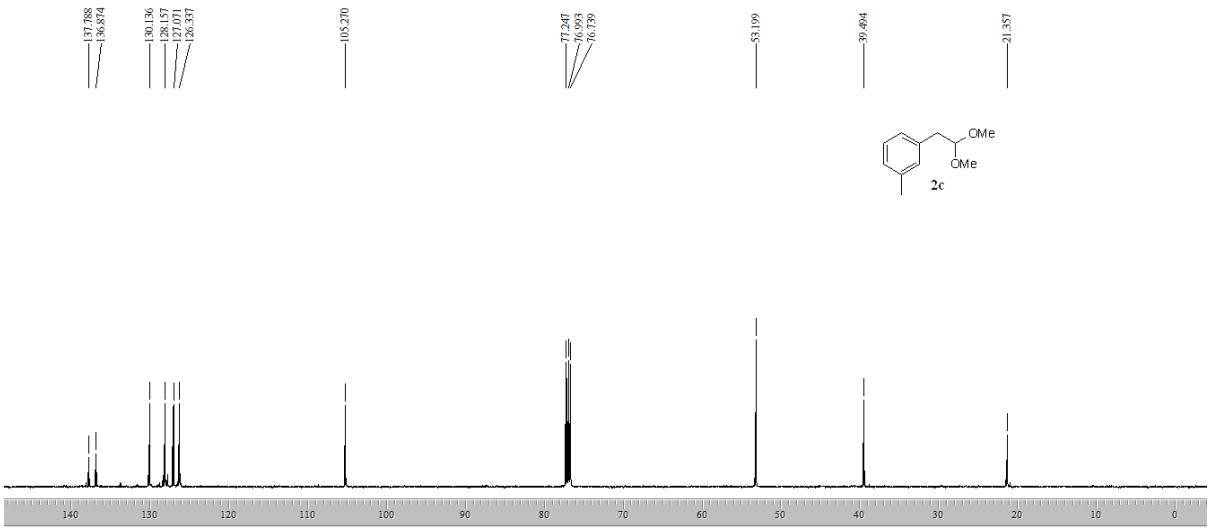

Figure S21

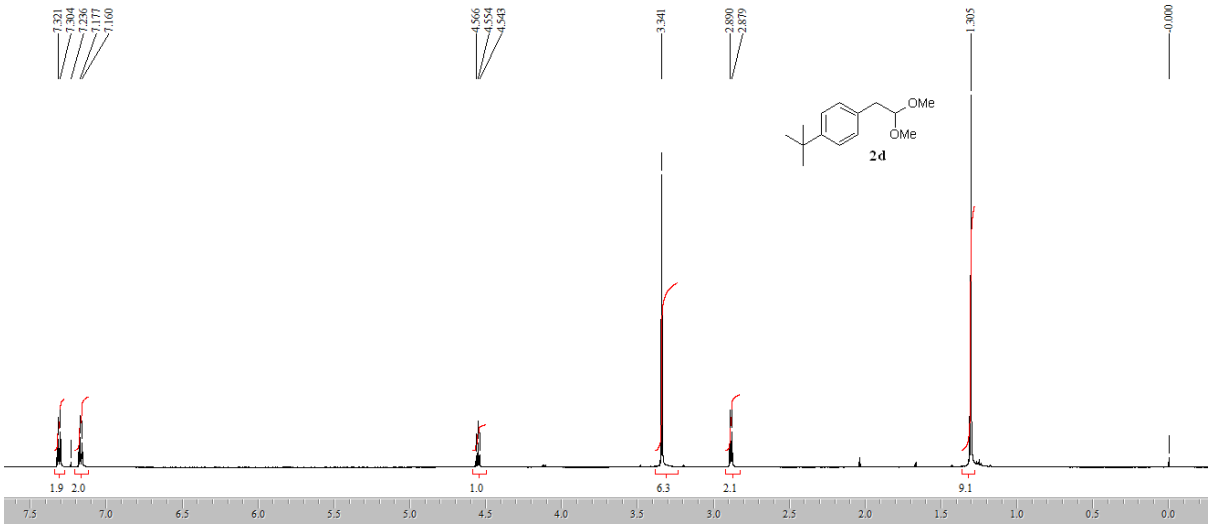

Figure S22

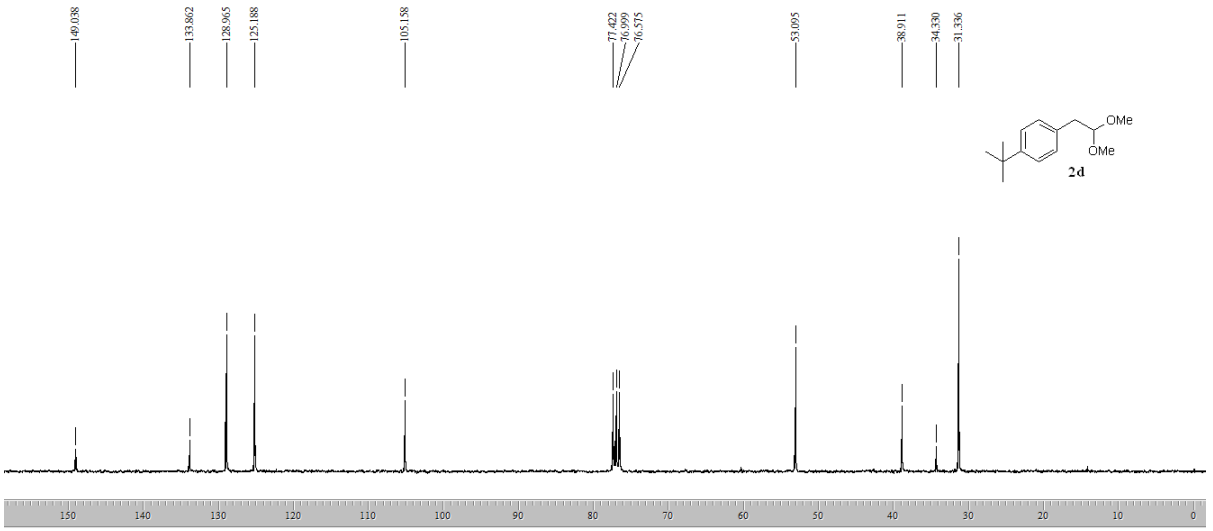

Figure S23

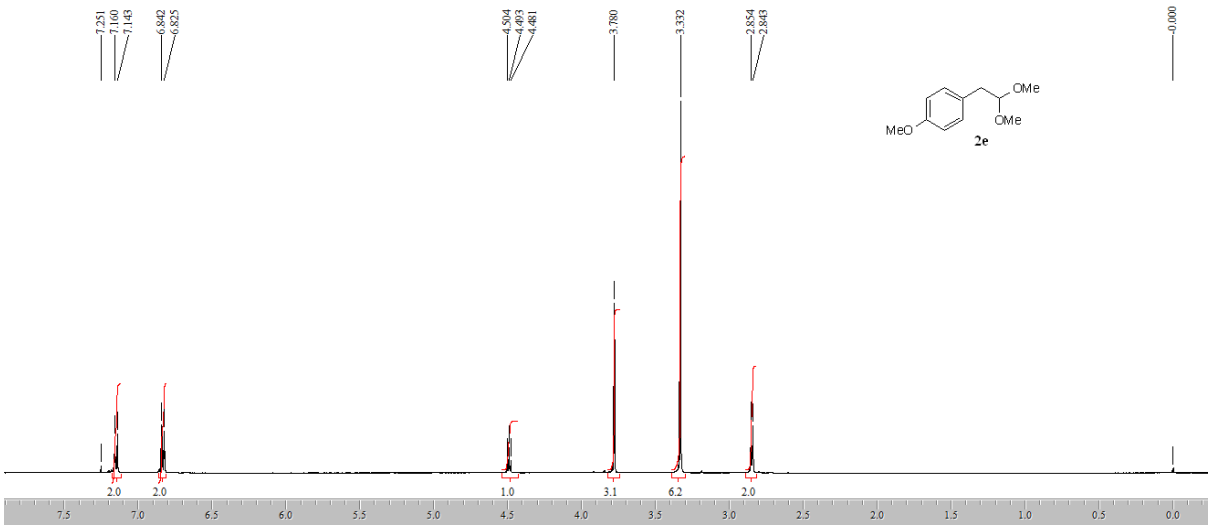

Figure S24

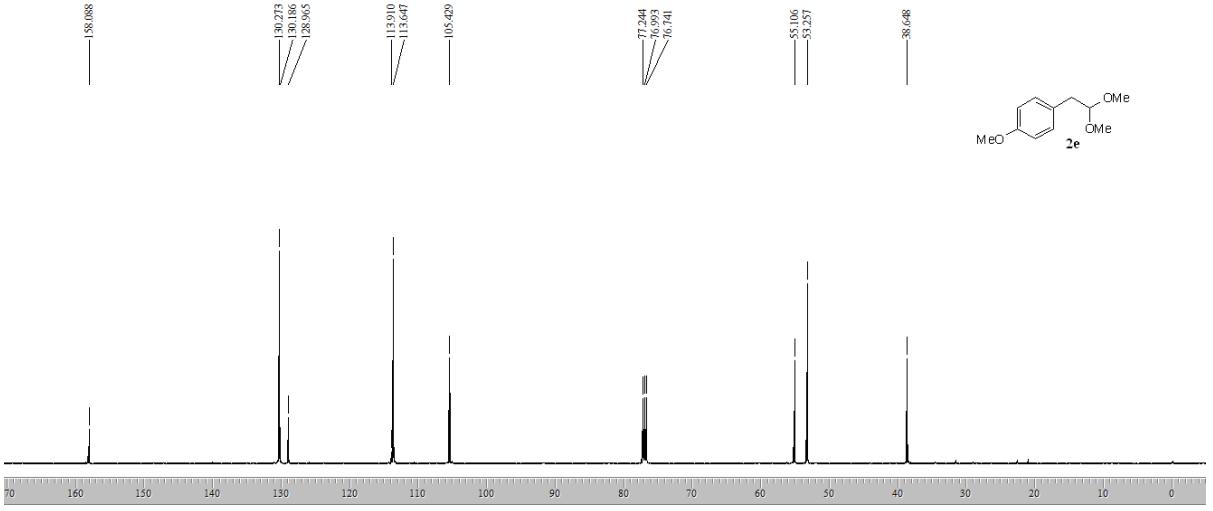

Figure S25

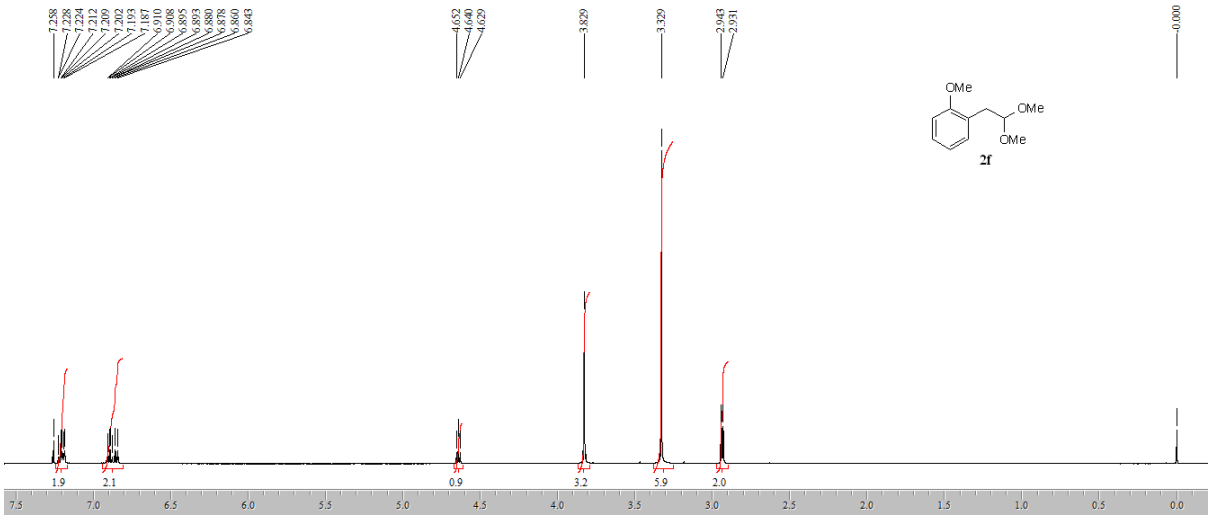

Figure S26

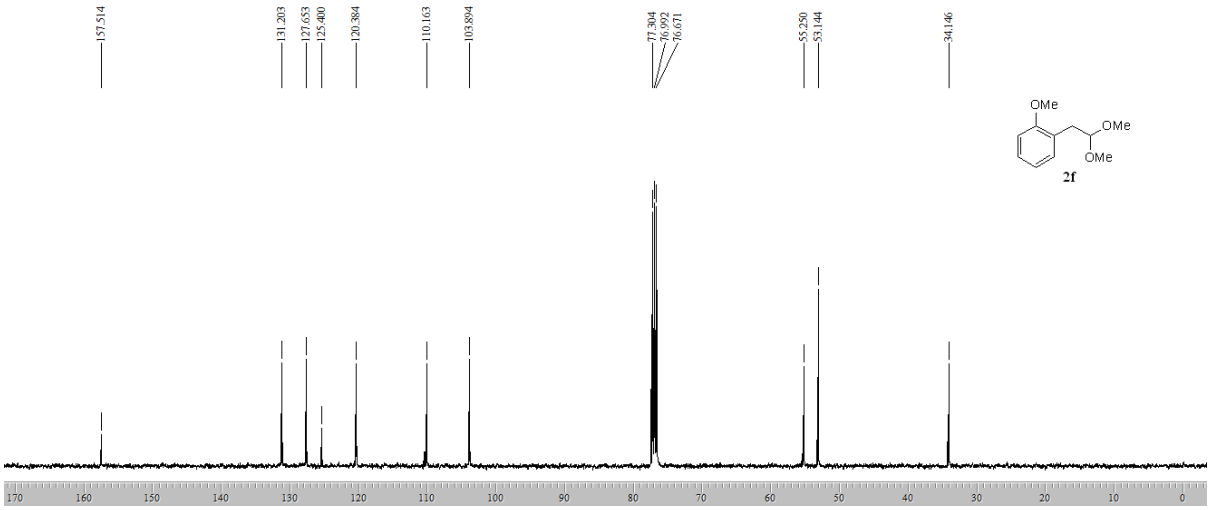

Figure S27

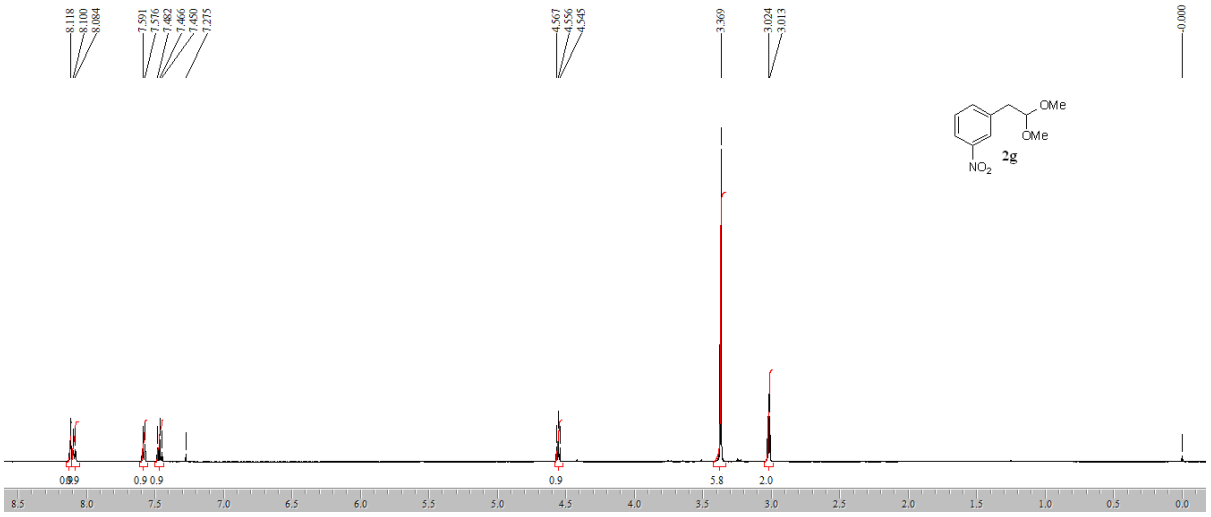

Figure S28

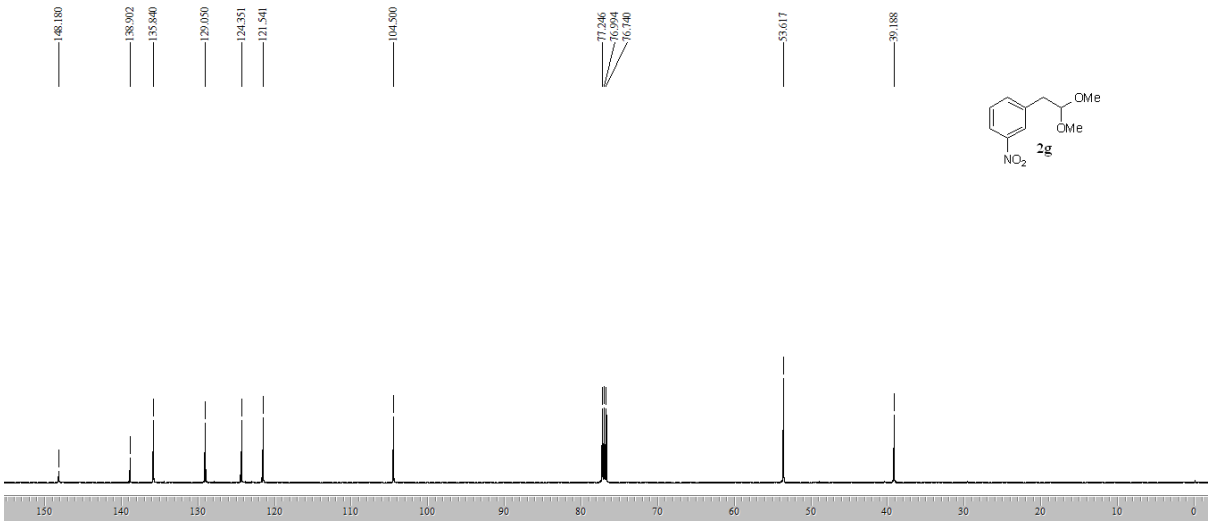

Figure S29

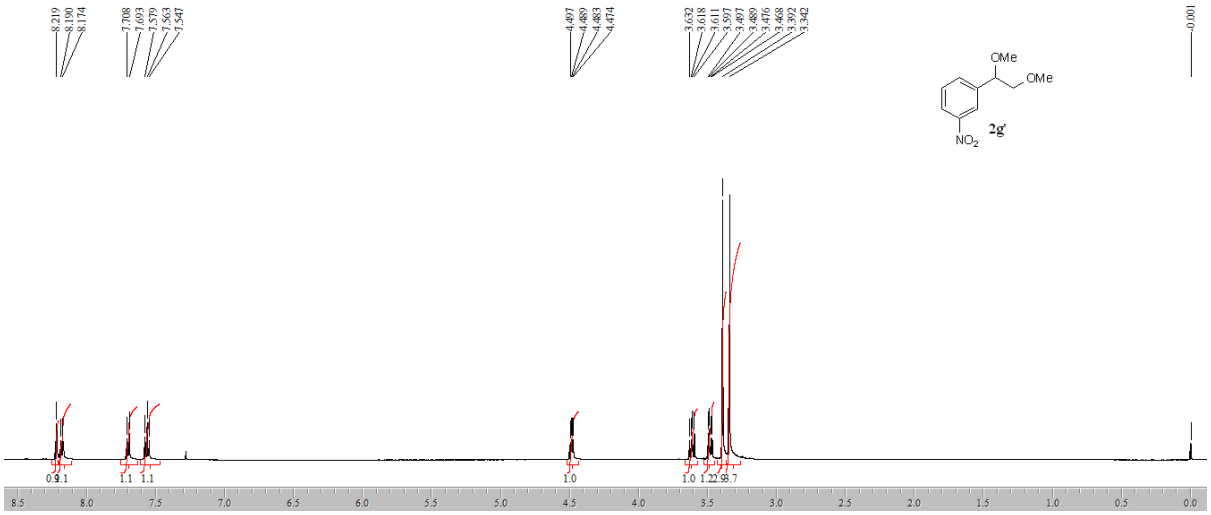

Figure S30

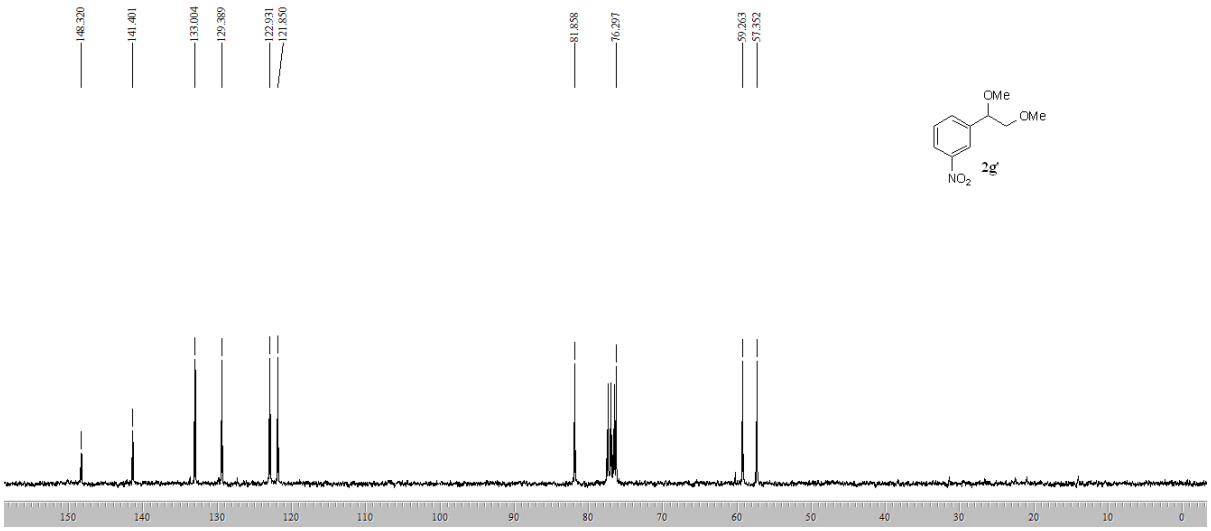

Figure S31

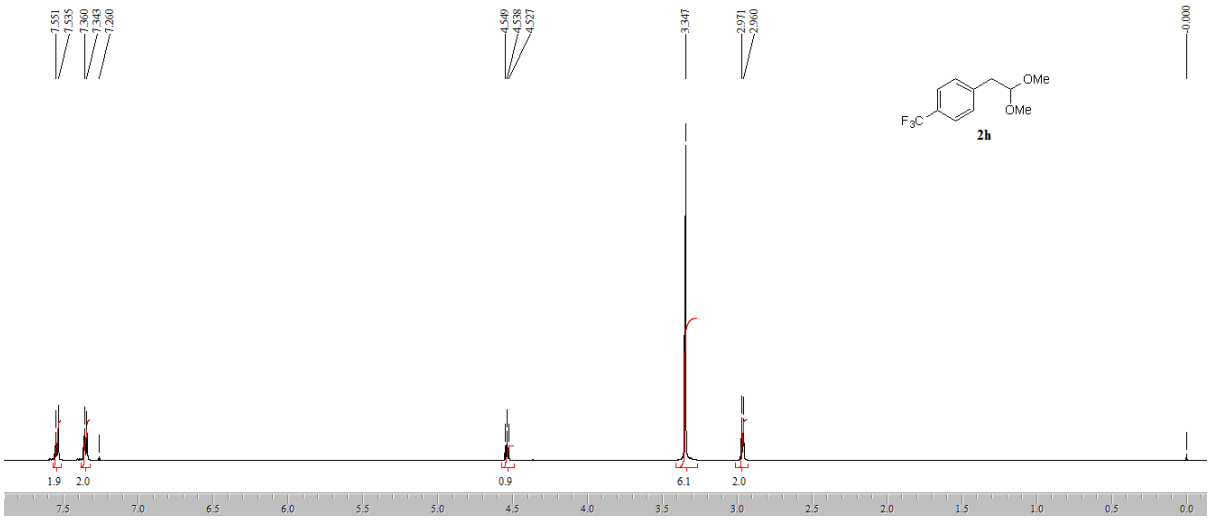

Figure S32

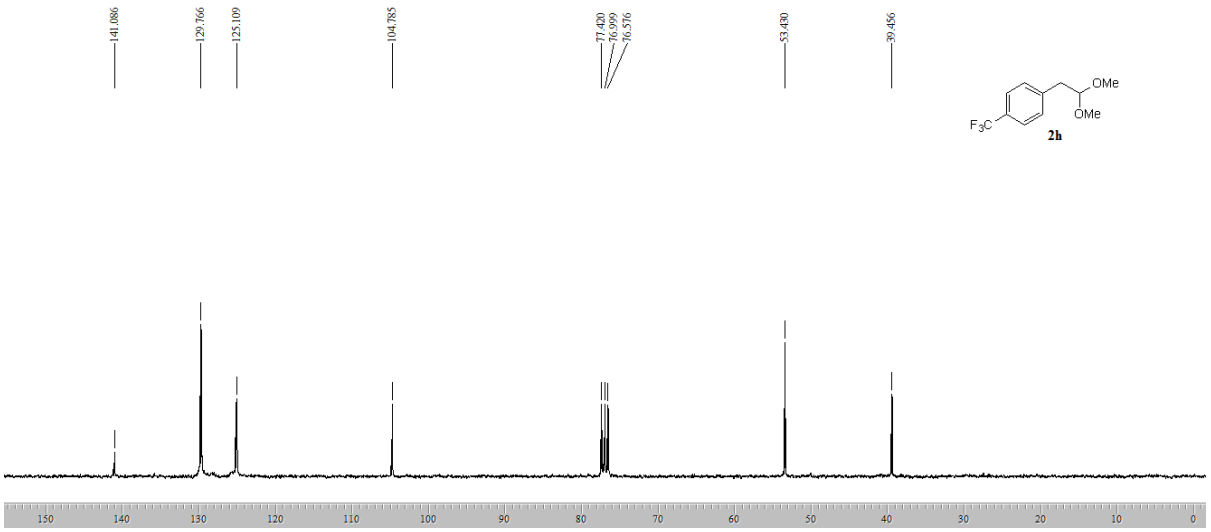

Figure S33

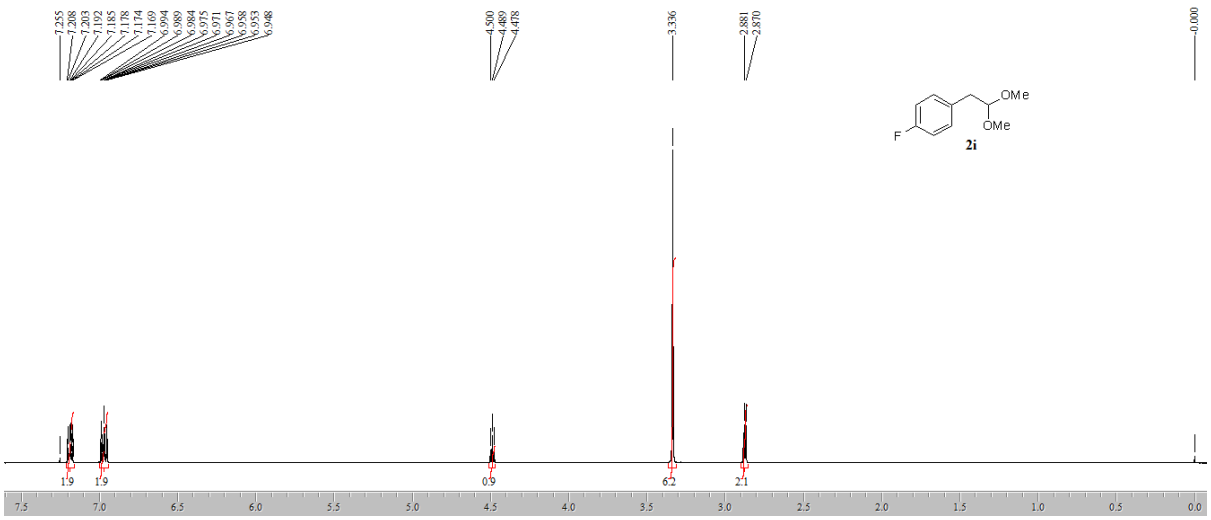

Figure S34

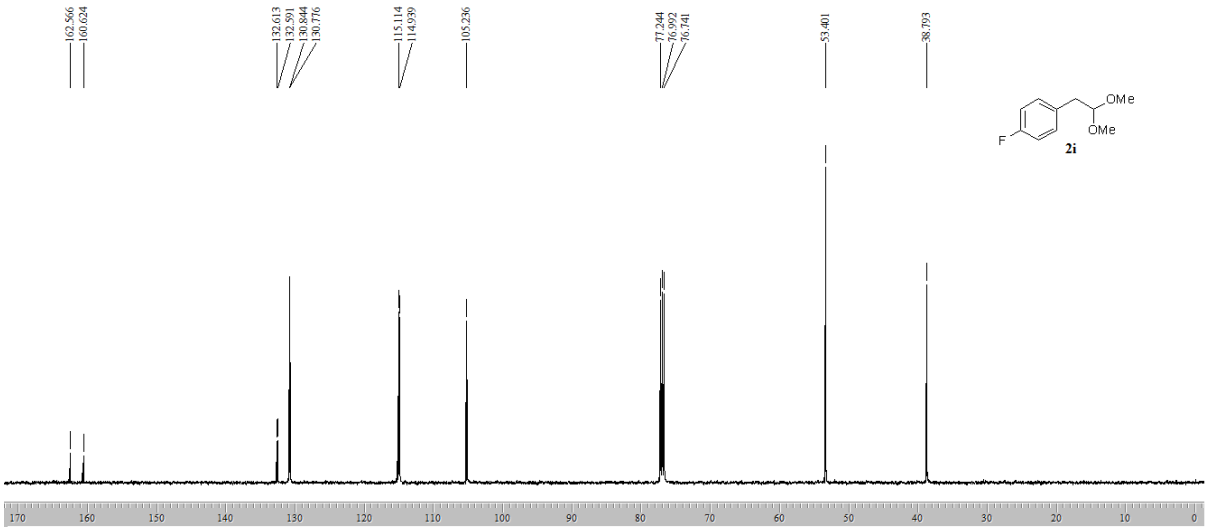

Figure S35

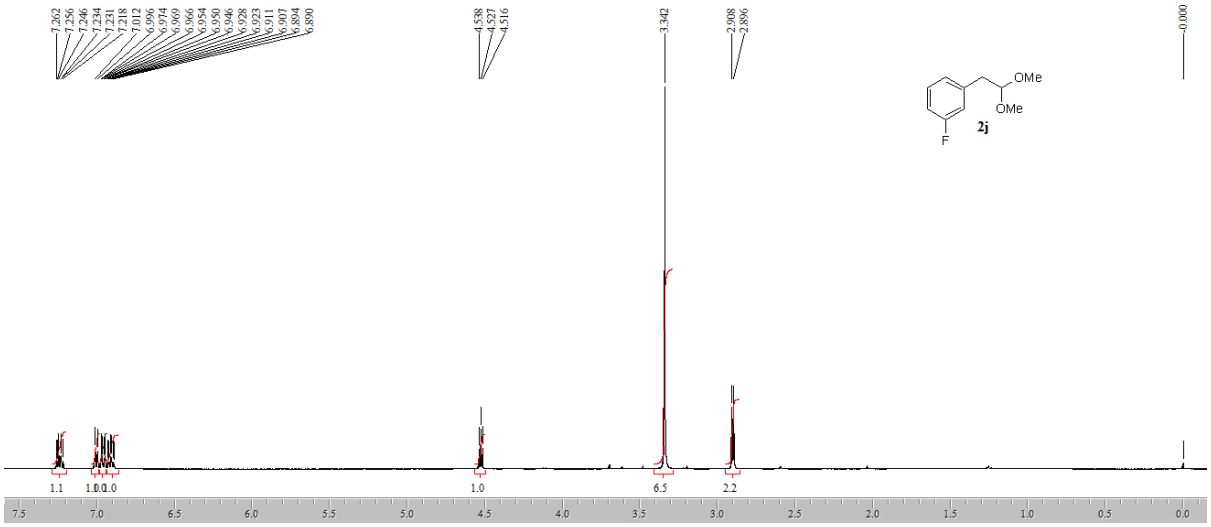

Figure S36

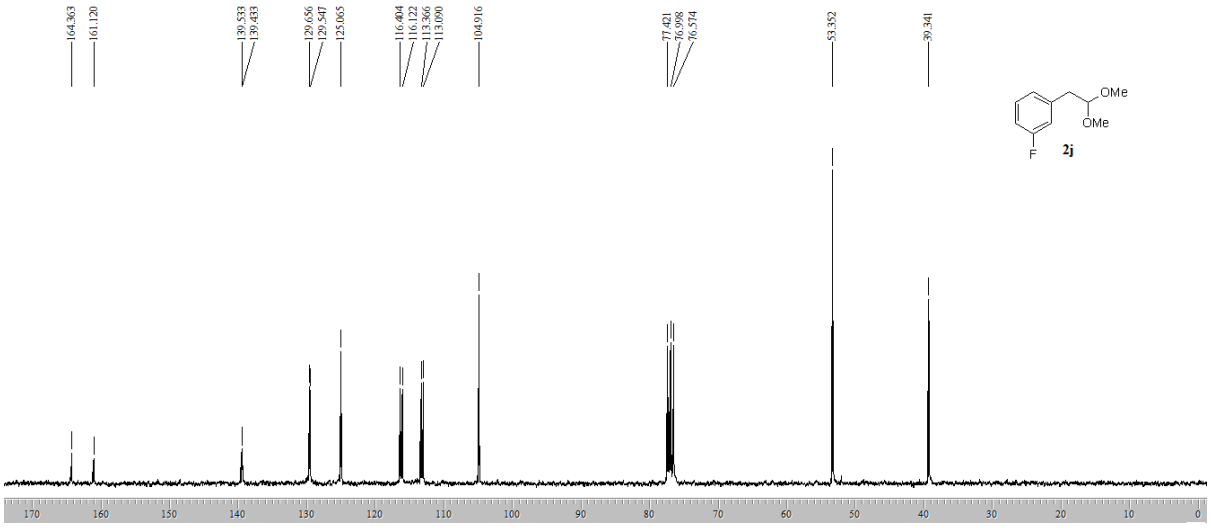

Figure S37

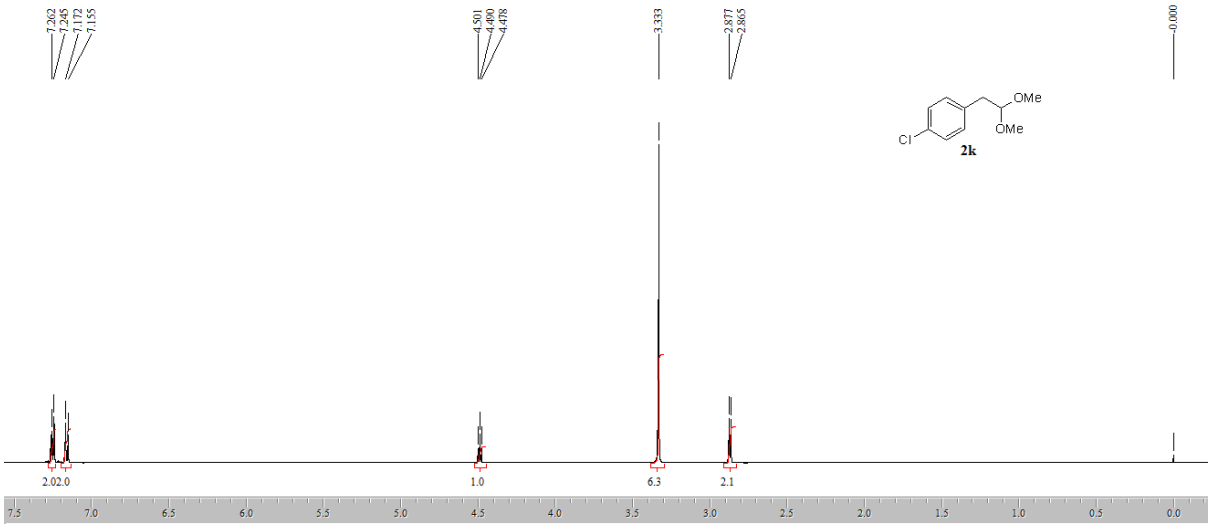

Figure S38

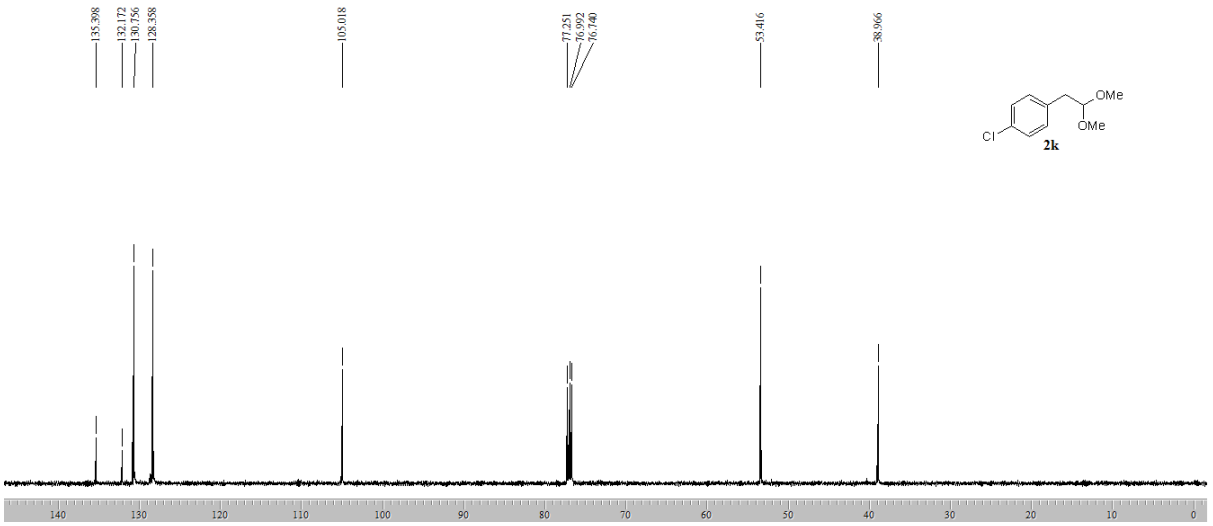

Figure S39

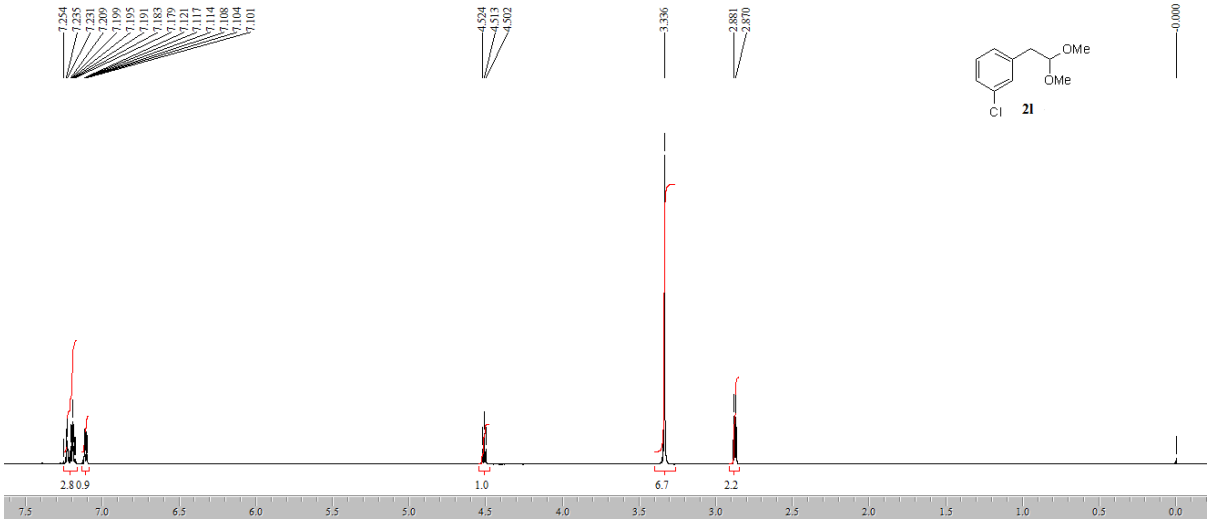

Figure S40

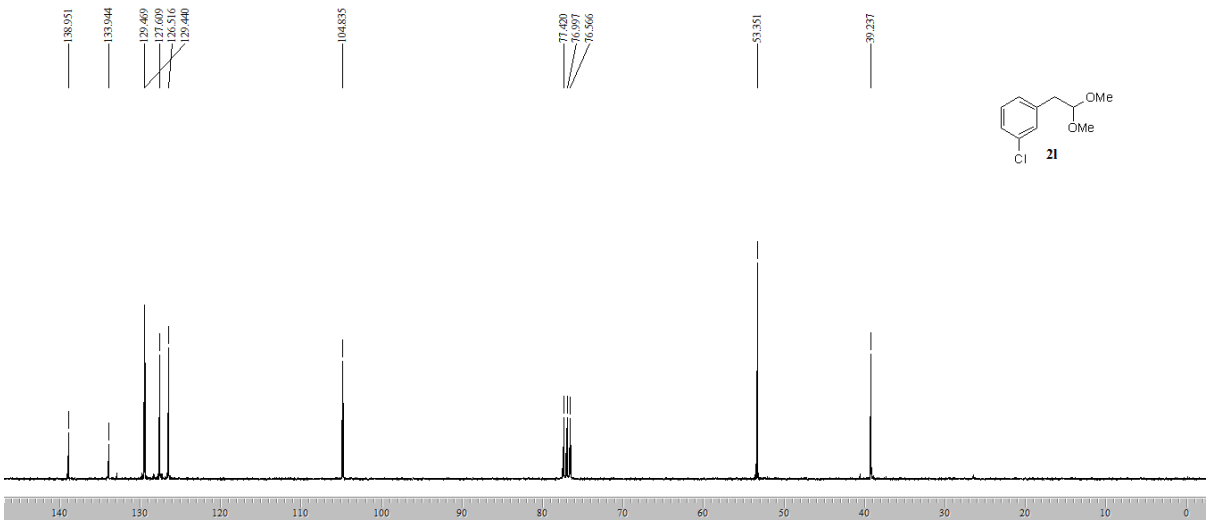

Figure S41

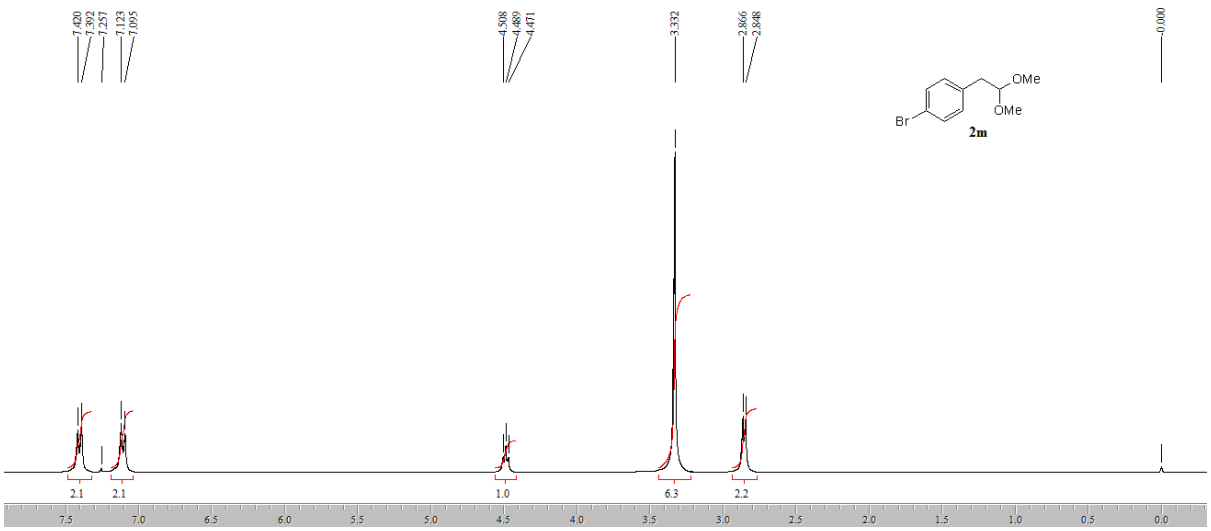

Figure S42

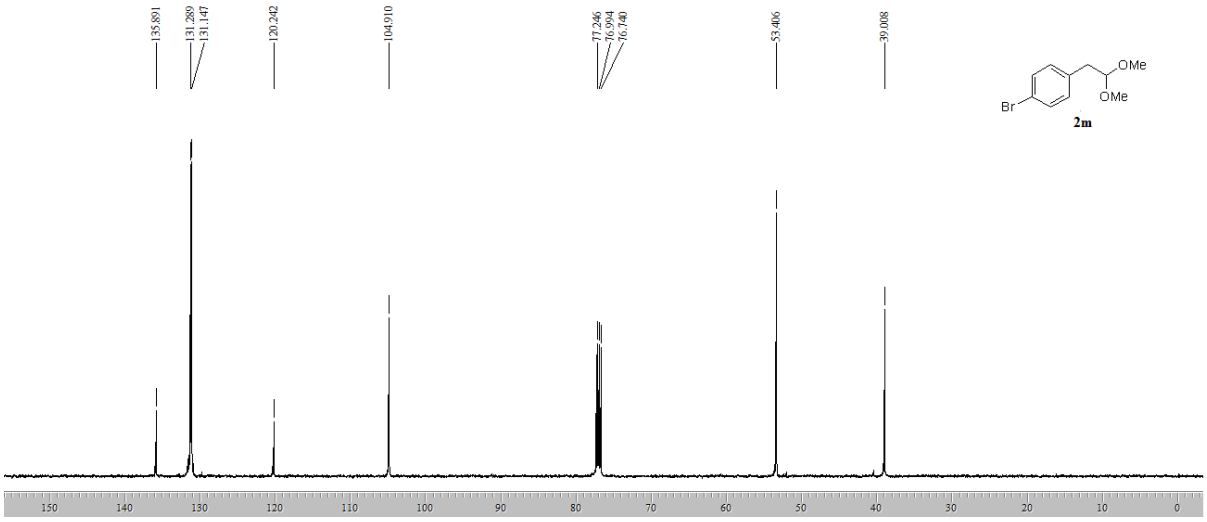

Figure S43

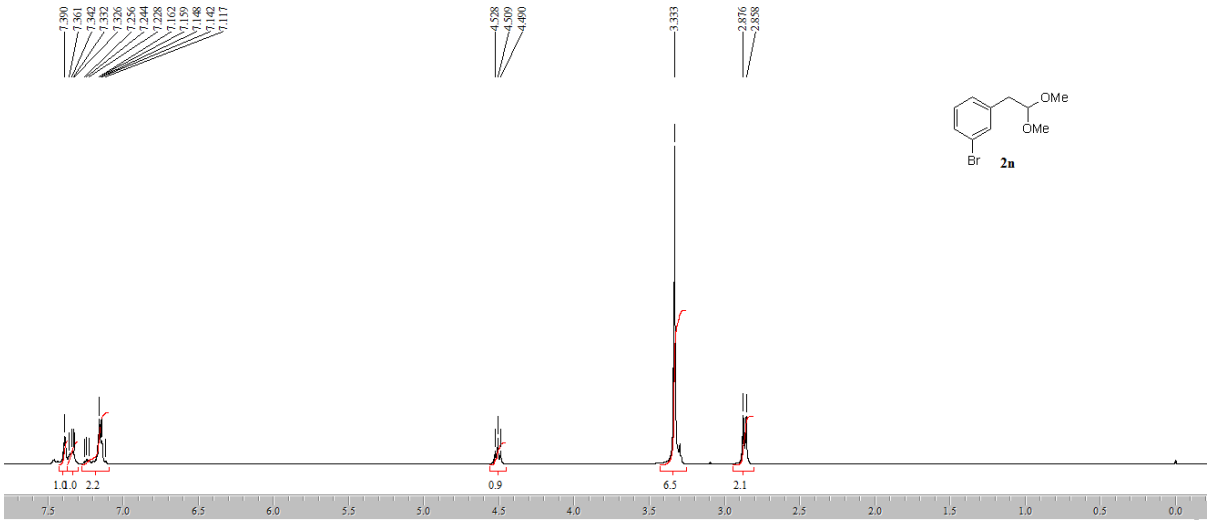

Figure S44

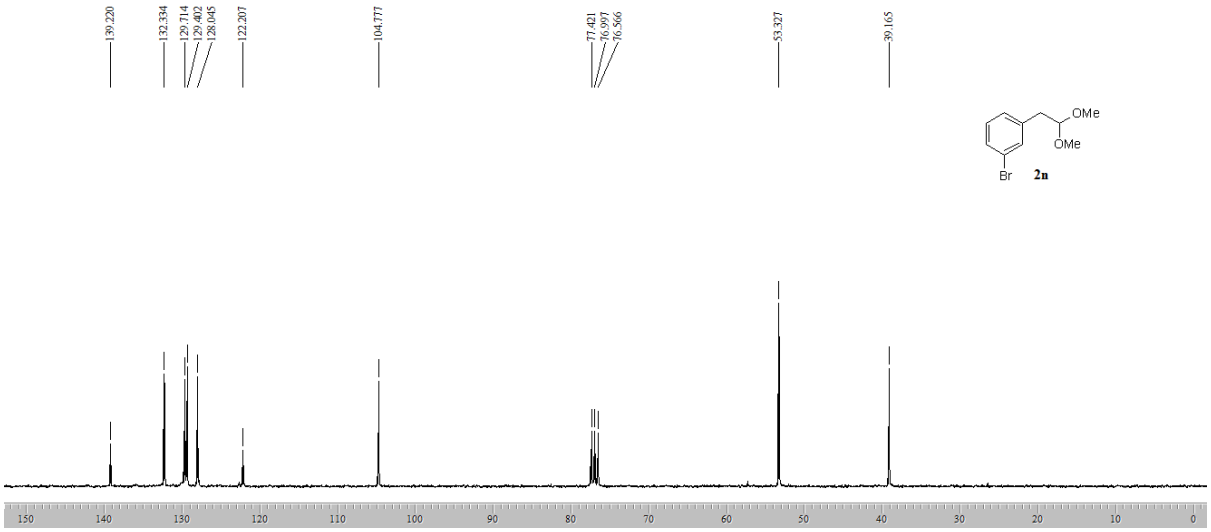

Figure S45

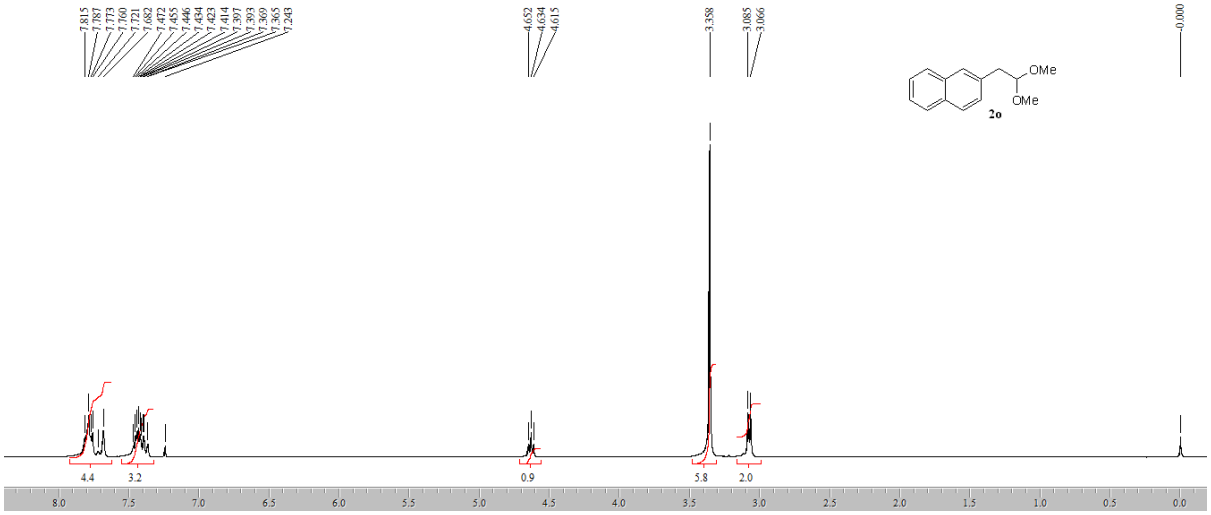

Figure S46

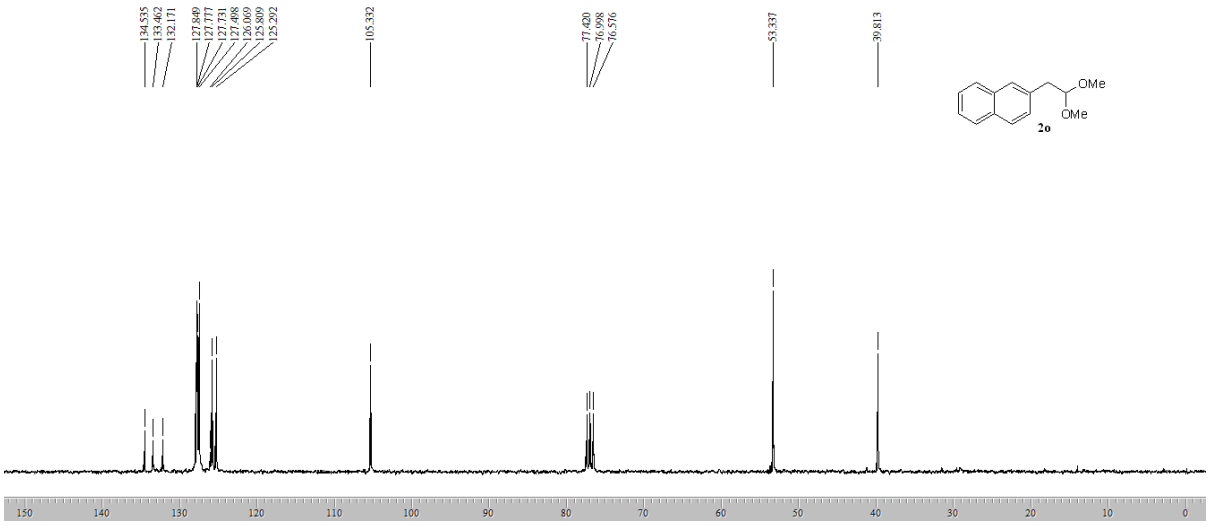

Figure S47

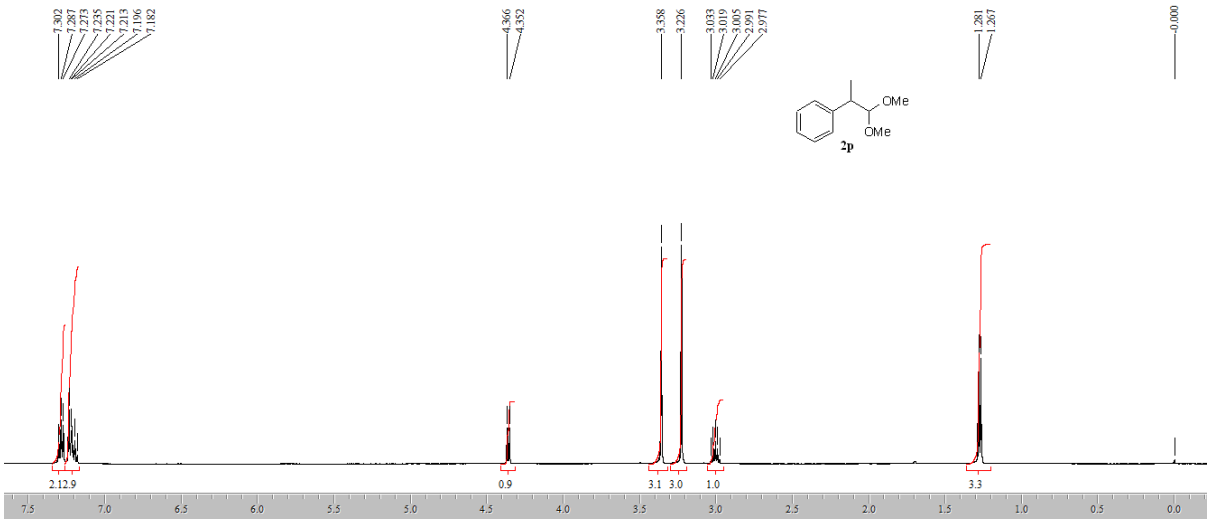

Figure S48

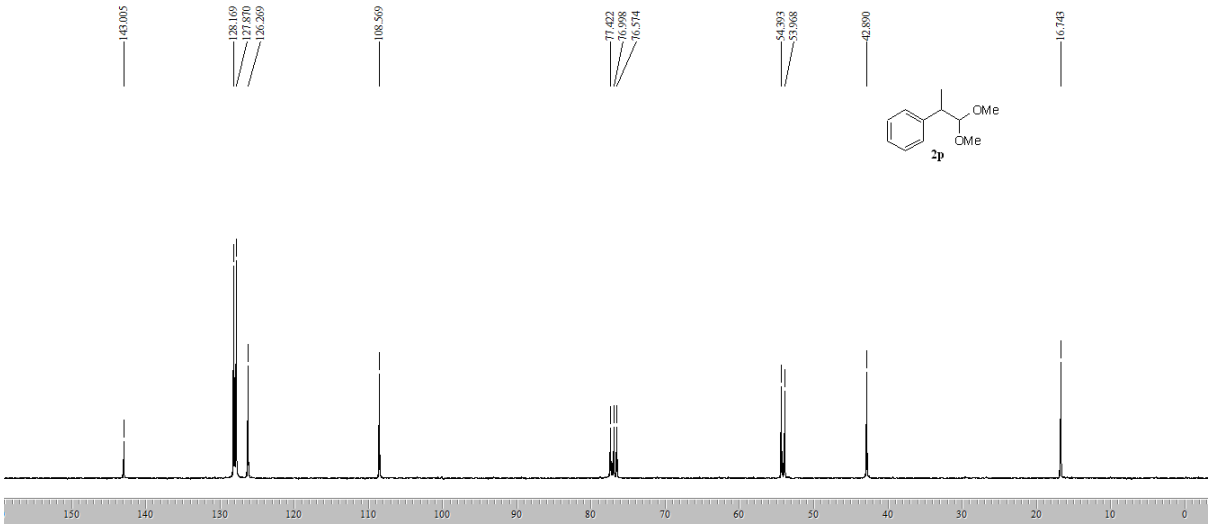

Figure S49

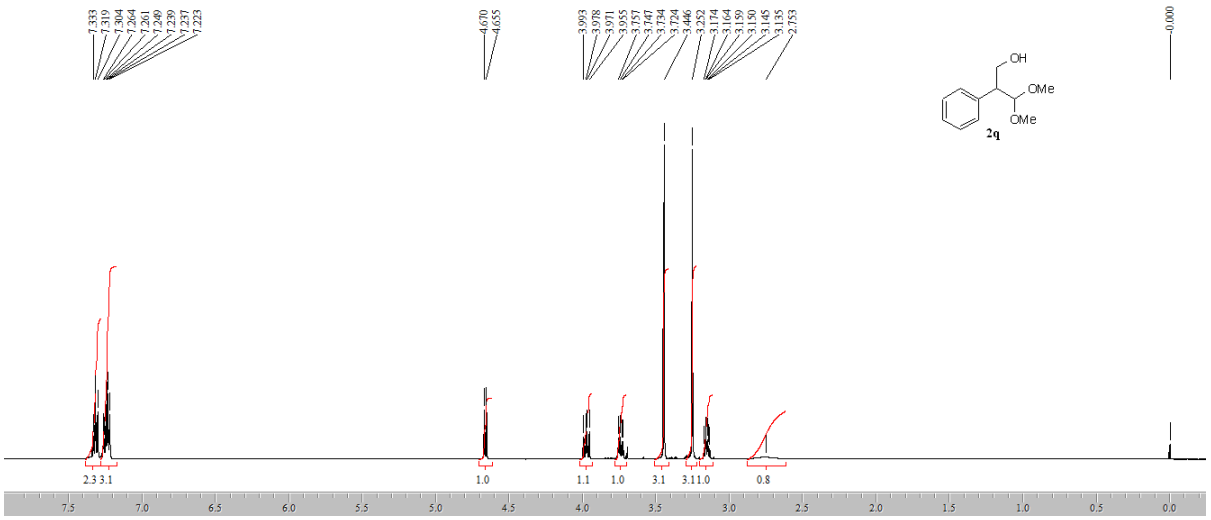

Figure S50

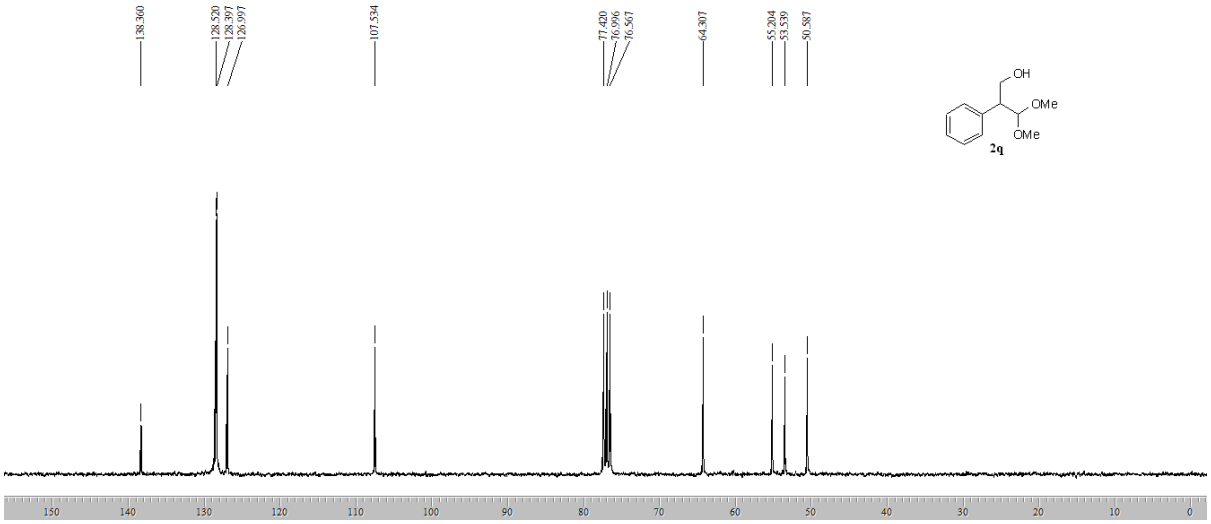

Figure S51

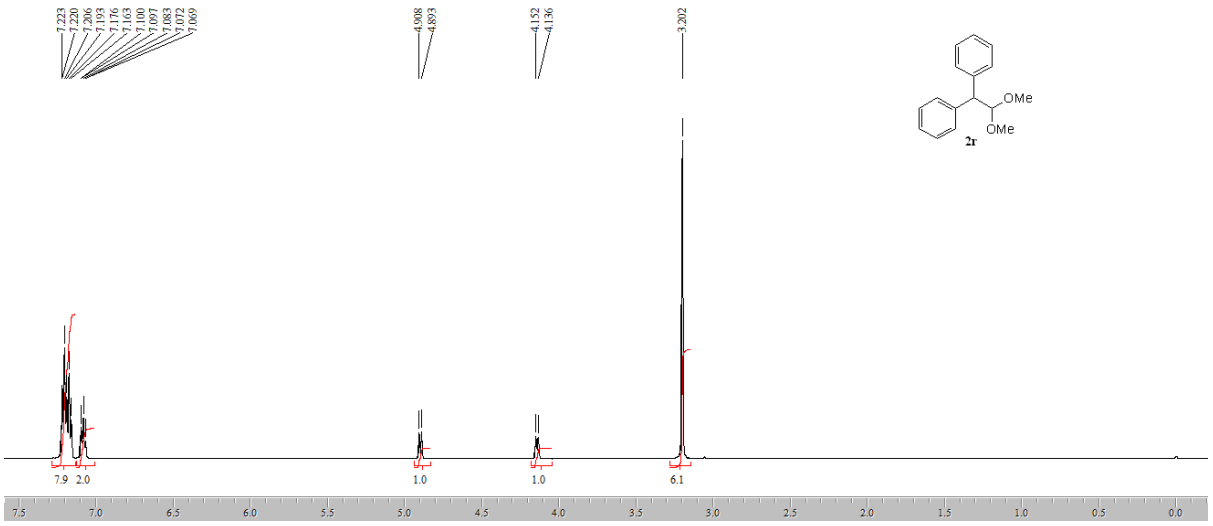

Figure S52

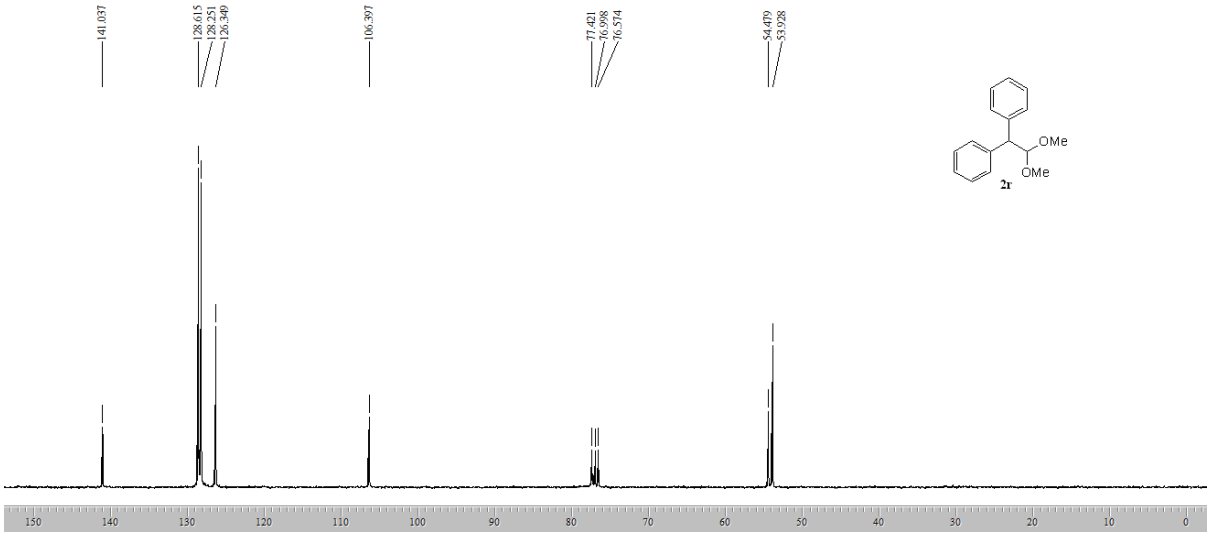

Figure S53

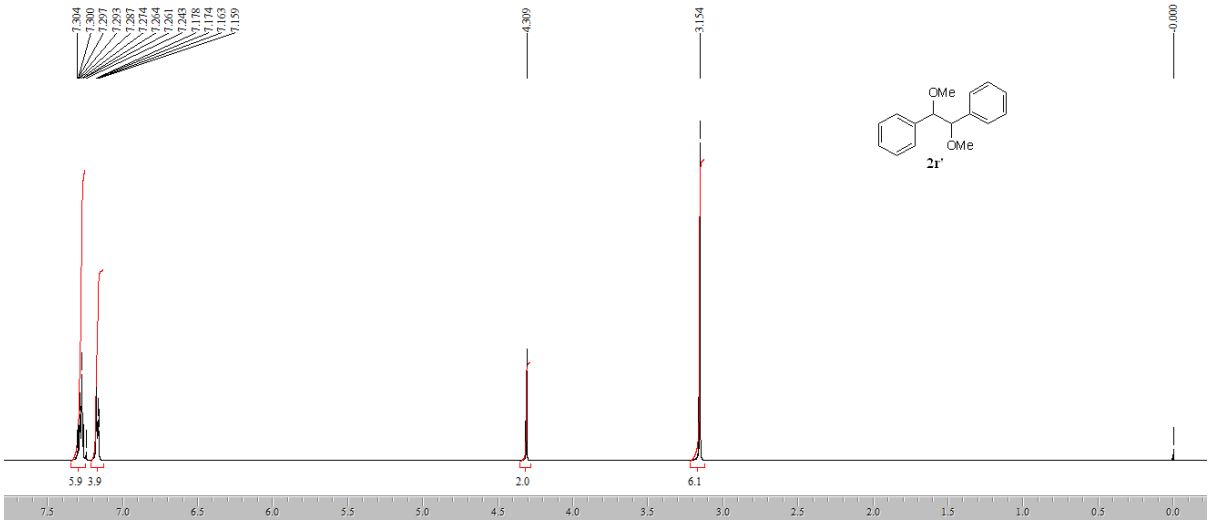

Figure S54

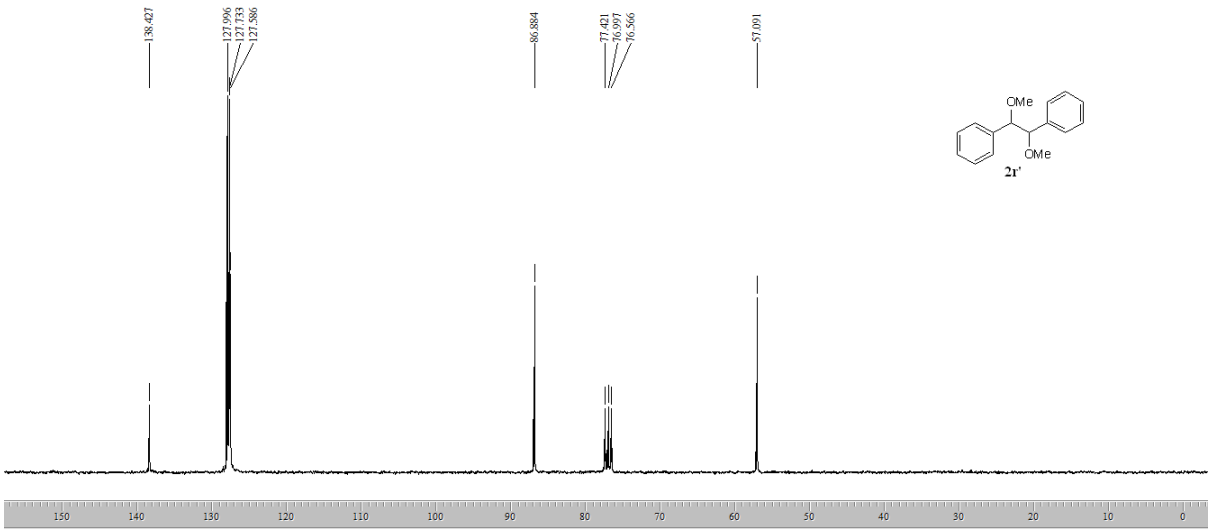

Figure S55

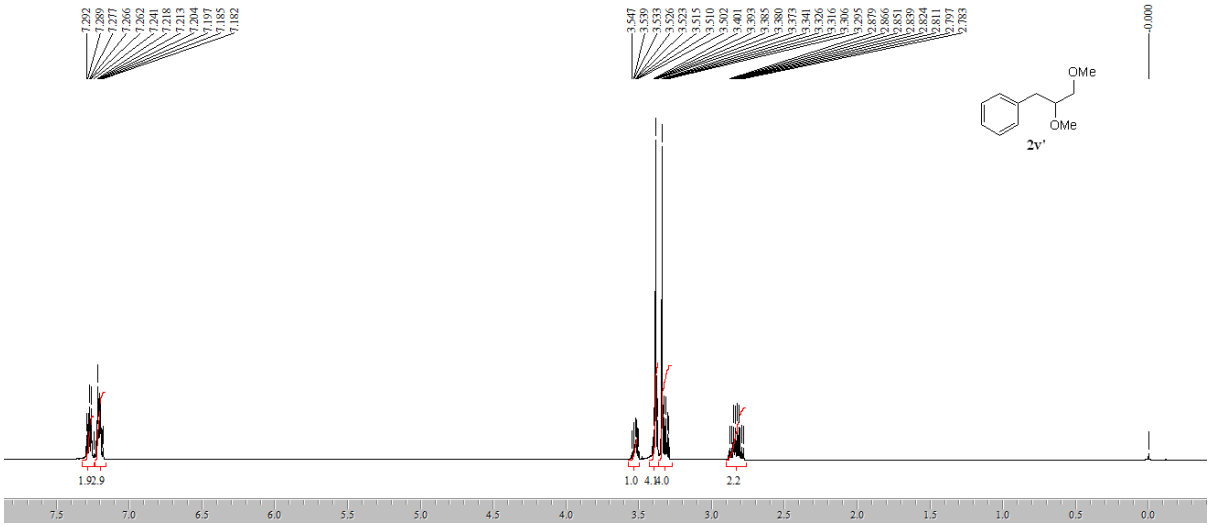

Figure S56

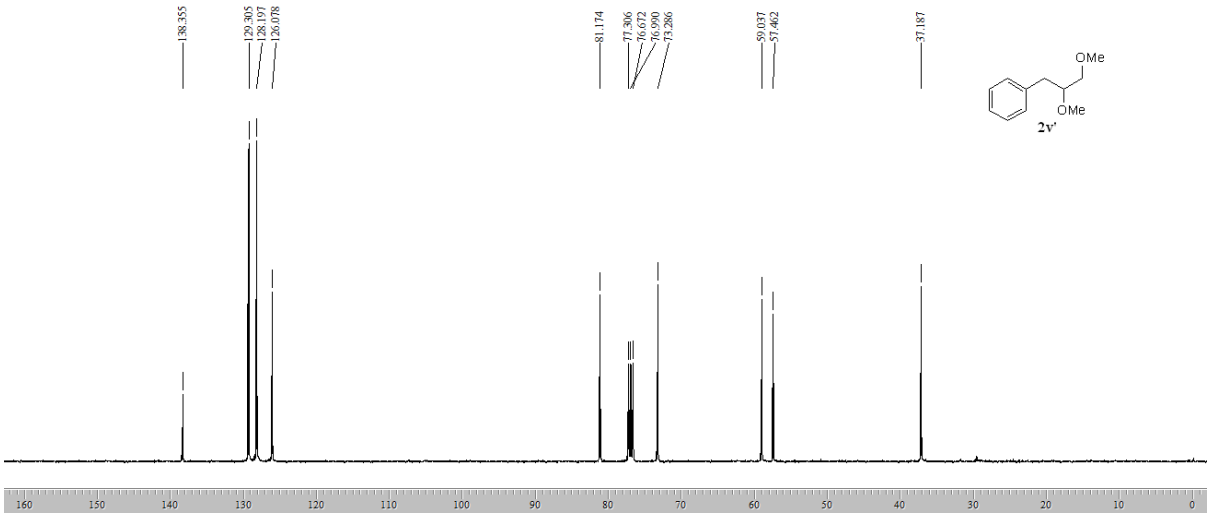

Figure S57

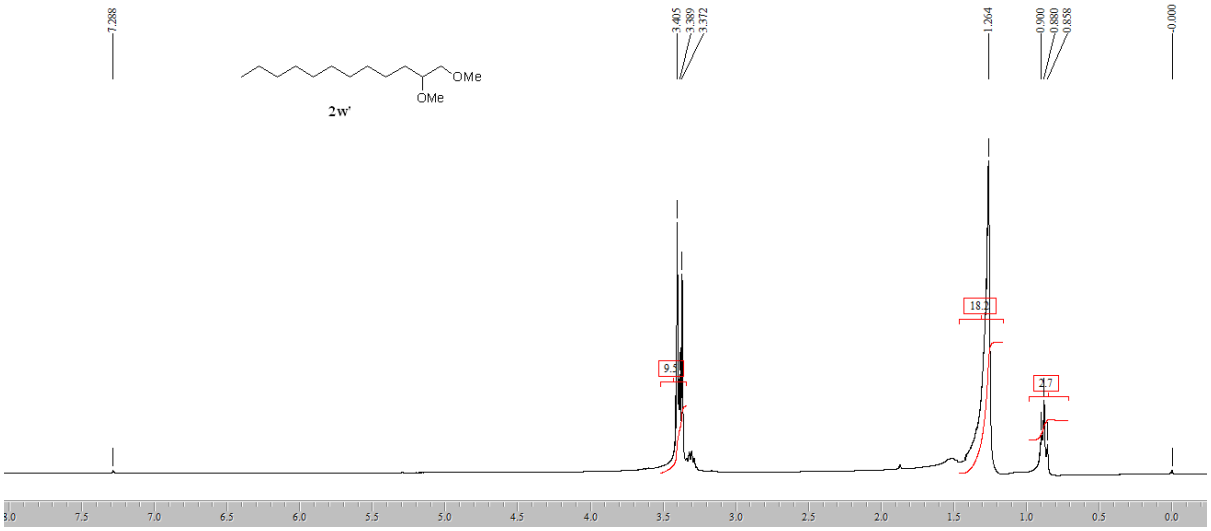

Figure S58

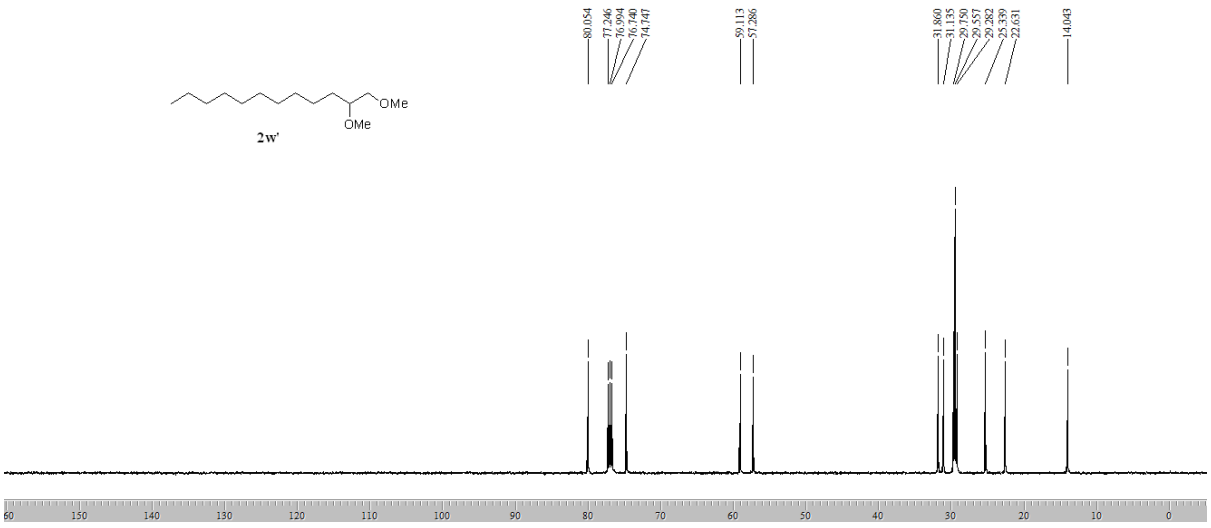

Figure S59

5. Notes and references

1. M. K. Agrawal, S. Adimurthy, B. Ganguly and P. K. Ghosh, *Tetrahedron,* 2009, **65**, 2791.
2. A. D. Chowdhury and G. K. Lahiri, *Chem. Commun.,* 2012, **48***,* 3448.
3. C. Zhu, Y. Zhang, H. Zhao, S. Huang, M. Zhang and W. Su, *Adv. Synth. Catal.,* 2015, **357**, 331.
4. TEMPO as radical inhibitor, *see*: (a) M. I. Guzmán, A. J. Colussi and M. R. Hoffmann, *J. Phys. Chem. A,* 2006, **110**, 3619; (b) P. Bałczewski and M. Mikołajczyk, *New J. Chem.* 2001, **25**, 659.
5. (a) P. Swamy, M. M. Reddy, M. Naresh, M. A. Kumar, K. Srujana, C. Durgaiah and N. Narender, *Adv. Synth. Catal.,* 2015, **357**, 1125; (b) A. Yoshimura, T. N. Jones, M. S. Yusubov and V. V. Zhdankin, *Adv. Synth. Catal.,* 2014, **356**, 3336; (c) S. Tang, Y. Wu, W. Liao, R. Bai, C. Liua and A. Lei, *Chem. Commun.,* 2014, **50**, 4496; (d) A. Yoshimura, C. Zhu, K. R. Middleton, A. D. Todora, B. J. Kastern, A. V. Maskaev and V. V. Zhdankin, *Chem. Commun.,* 2013, **49**, 4800; (e) U. Kloeckner, P. Finkbeiner and B. J. Nachtsheim, *J. Org. Chem.,* 2013, **78**, 2751.
6. F. J. Fañanás, M. Álvarez-Pérez and F. Rodríguez, *Chem. Eur. J.,* 2005, **11**, 5938.
7. (a) L. S. Santos, L. Knaack and J. O. Metzger, *Int. J. Mass Spectrom.,* 2005, **246**, 84; (b) M. N. Eberlin, *Eur. J. Mass Spectrom.,* 2007, **13**, 19; (c) L. S. Santos, *Eur. J. Org. Chem.,* 2008, 235.
8. (a) S. Meyer and J. O. Metzger, *Anal. Bioanal. Chem.,* 2003, **377**, 1108; (b) S. Fürmeier and J. O. Metzger, *J. Am. Chem. Soc.,* 2004, **126**, 14485; (c) L. S. Santos, C. H. Pavam, W. P. Almeida, F. Coelhoand and M. N. Eberlin, *Angew. Chem.,* 2004, **116**, 4430; *Angew. Chem. Int. Ed.,* 2004, **43**, 4330; (d) X. Zhang, Y. Liao, R. Qian, H. Wang and Y. Guo, *Org. Lett.,* 2005, **7**, 3877; (e) C. Marquez and J. O. Metzger, *Chem. Commun.,* 2006, 1539; (f) J. Roithová and D. Schrçder, *Chem. Eur. J.,* 2008, **14**, 2180.
9. W. W. Y. Lam, W.-L. Man, Y.-N. Wang and T.-C. Lau, *Inorg. Chem.,* 2008, **47**, 6771.
10. G. Lente, J. Kalmár, Z. Baranyai, A.z Kun, I. Kék, D. Bajusz, M. Takács, L. Veres and I. Fábián, *Inorg. Chem.,* 2009, **48**, 1763.
11. D. A. Palmer and R. van Eldik, *Inorg. Chem.,* 1986, **25**, 928.
12. L. Nadon, M. Tardat, M. Zador and S. Fliszar, *Can. J. Chem.,* 1973, **51**, 2366.
13. A. M. Balija, K. J. Stowers, M. J. Schultz and M. S. Sigman, *Org. Lett.,* 2006, **8**,

1121.

14. M. Tiecco, L. Testaferri, M. Tingoli, D. Chianelli and D. Bartoli, *Tetrahedron,* 1988, **44**, 2261.